

**A NOVEL NON-GLUCOSE BASED OSMOTIC AGENT WITH LIVER UPTAKE
POTENTIAL FOR PERITONEAL DIALYSIS SOLUTIONS**

by

Meenakshi Swaminathan

B.Tech., SASTRA University, 2016

A THESIS SUBMITTED IN PARTIAL FULFILLMENT OF
THE REQUIREMENTS FOR THE DEGREE OF

MASTER OF SCIENCE

in

THE FACULTY OF GRADUATE AND POSTDOCTORAL STUDIES
(EXPERIMENTAL MEDICINE)

THE UNIVERSITY OF BRITISH COLUMBIA

(Vancouver)

June 2021

© Meenakshi Swaminathan, 2021

The following individuals certify that they have read, and recommend to the Faculty of Graduate and Postdoctoral Studies for acceptance, the thesis entitled:

A novel non-glucose based osmotic agent with liver uptake potential for peritoneal dialysis solutions submitted by Meenakshi Swaminathan in partial fulfillment of the requirements for the degree of Master of Science in Experimental Medicine.

Examining Committee:

Dr. Caigan Du, Associate Professor, Department of Urologic Sciences, UBC
Supervisor

Dr. Jayachandran Kizhakkedathu, Professor, Department of Laboratory Medicine and Pathology, UBC
Co-supervisor

Dr. Dirk Lange, Associate Professor, Department of Urologic Sciences, UBC
Supervisory Committee Member

Dr. Christopher Ong, Associate Professor, Department of Urologic Sciences, UBC
Additional Examiner

Abstract

Peritoneal Dialysis (PD), a treatment modality for end-stage renal disease (ESRD) uses high concentrations of glucose in its dialysis solutions. Since, 40% ESRD patients are diabetic, use of glucose-based PD solutions is non-rational because of the local and systemic adverse effects of glucose. There is a need for a biocompatible, non-glucose based osmotic agent that can replace glucose in peritoneal dialysis solutions. Recent studies on low molecular weight hyperbranched polyglycerol (HPG) as an osmotic agent show good ultrafiltration and reduction of peritoneal membrane injury but elimination through the kidneys. Our studies show that HPG is excreted via kidneys, and in ESRD patients, kidney function is impaired which could potentially result in poor excretion of this osmotic agent. N-acetylgalactosamine (GalNAc) carrying proteins and macromolecules has shown to be effectively up taken by the liver through asialoglycoprotein receptor (ASGPR). Thus, we hypothesize that HPG modified by GalNAc conjugation can be recognized by ASGPR in the liver, taken up and excreted through feces. GalNAc epoxide was synthesized by standard organic modifications and conjugated with HPG (3K) at two different densities (one or three GalNAc molecules per HPG) (denoted as HPG+1S or HPG+3S). The polymers were labeled with alexa647 and screened for effective internalization in a panel of hepatocyte cell lines with different levels of ASGPR expression using flow cytometry. Results of dose-dependent uptake of polymers and ASGPR staining of hepatocytes suggested receptor mediated internalization of HPG+3S in HepG2 and HuH7.5.1 cells. K_m values were assessed to determine the efficacious HPG conjugate followed by competitive inhibition with natural ligands of ASGPR in HepG2 cells. HEK293 cells ectopically expressing ASGPR1 and ASGPR1&2 genes were used to confirm HPG+3S uptake through ASGPR specifically. Mice tissue distribution studies of radiolabeled HPG and

HPG+3S showed better uptake of HPG+3S by the liver than HPG. Percentage of HPG+3S excreted via feces was significantly more than HPG in mice with normal kidney function, which support the enhanced binding of HPG+3S to ASGPR in hepatocytes. In conclusion, both our in vitro and in vivo results substantiate our claim that GalNAc conjugated HPG can be rerouted to be excreted via feces.

Lay Summary

About 40% of kidney failure patients cannot opt for peritoneal dialysis because they are diabetic and peritoneal dialysis solutions contain high concentrations of glucose. Hyperbranched Polyglycerol (HPG) has been proven to be safe with properties good enough to replace glucose in peritoneal dialysis solutions but show poor excretion when kidney function is compromised. We suggest modification of HPG with GalNAc that target the liver and eventually be excreted through feces. We made a few HPG-GalNAc polymers which were tested in liver cells and the better performing polymer was tagged and injected into mice. HPG-GalNAc polymers showed better uptake in both liver cells and mice liver than HPG. Mice were able to excrete HPG-GalNAc through feces despite having normal kidney function. Further studies on HPG-GalNAc need to be performed to test its ability as an osmotic agent in peritoneal dialysis.

Preface

Most of the work for this study was conducted by Meenakshi Swaminathan under the supervision of Dr. Caigan Du at The University of British Columbia. Synthesis, characterization, and labeling of polymer was performed with a lot of help and guidance from Ms. Irina Chafeeva and Dr. Srinivas Abbina under the supervision of Dr. Jaychandran Kizhakkedathu at Centre for Blood Research, UBC. The in vitro work and analysis were carried out by Meenakshi Swaminathan with guidance from Ms. Qiunong Guan at Jack Bell Research Centre, Vancouver General Hospital Campus. The in vivo work was performed by the Investigational Drug Program team led by Ms. Nicole Wretham under supervision from Dr. Nancy Dos Santos at Experimental Therapeutics and Animal Resource Centre, BC Cancer Research Centre, Vancouver. Analysis of in vivo data was performed by Meenakshi Swaminathan with guidance from Dr. Srinivas Abbina.

Ethics approval for in vivo studies was obtained from the UBC Animal Care Committee and the certificate number is **A18-0276**.

Table of Contents

Abstract	iii
Lay Summary	v
Preface	vi
Table of Contents	vii
List of Tables	x
List of Figures	xi
List of Symbols	xiv
List of Abbreviations	xv
Glossary	xvii
Acknowledgements	xviii
Dedication	xx
Chapter 1: Introduction	1
1.1 End Stage Renal Disease.....	2
1.2 Dialysis.....	2
1.3 Peritoneal Dialysis:	3
1.4 Hyperbranched Polyglycerol (HPG):.....	8
1.5 Asialoglycoprotein Receptor (ASGPR):.....	12
Chapter 2: Objective of the thesis	15
Chapter 3: Materials and Methods	16
3.1 HPG-GalNAc Synthesis.....	16
3.1.1 Step 1: Synthesis of Galactopyrano-2-oxazoline	16

3.1.2	Step 2: Gal-2-oxazoline to Allyl-GalNAc.....	17
3.1.3	Step 3: Allyl-GalNAc to GalNAc-epoxide	18
3.1.4	Step 4: Conjugation of HPG-3K with GalNAc-epoxide.....	19
3.2	Labelling of polymer conjugates.....	20
3.2.1	Alexa 647 labelling	21
3.2.2	Radiolabeling	21
3.3	In vitro: Cell Culture	21
3.3.1	Initial screening of polymer conjugate internalization.....	22
3.3.2	Receptor Mediated Internalization.....	23
3.3.2.1	ASGPR expression in the panel of hepatocyte cultures.....	24
3.3.2.2	Determination of affinity of the polymer conjugates.....	24
3.3.2.3	Internalization by HEK293 Cells Ectopically Expressing ASGPR	25
3.3.2.4	Competitive Inhibition of HPG+3S with Natural Ligands	26
3.3.3	Efflux of HPG+3S from Hepatocytes	27
3.3.4	Internalization of the conjugate in other cells expressing ASGPR.....	27
3.4	In vivo – Bio Distribution of HPG and HPG+3S in C57Bl/6 mice.....	28
3.5	Statistical analysis	29
Chapter 4: Results.....		30
4.1	Characterization of HPG polymers	30
4.2	In vitro examination of HPG and GalNAc conjugated HPG	33
4.2.1	Initial screening of polymer internalization in different hepatocyte cell lines.	33
4.2.2	Receptor mediated internalization of HPG+3S.....	36
4.2.2.1	ASGPR expression in different human hepatocyte cell lines.	36

4.2.2.2	Determination of affinity of polymer conjugates and dose dependent internalization.....	37
4.2.2.3	Uptake in Kidney Cells that Ectopically Express ASGPR	41
4.2.2.4	Competitive Inhibition with Natural Ligands	42
4.2.3	Efflux of HPG+3S from Hepatocytes	45
4.2.4	Internalization by Monocytes.....	46
4.3	Biodistribution of HPG and HPG+3S in mice	48
4.3.1	Digestive System.....	48
4.3.2	Urinary System	51
4.3.3	Circulatory System.....	53
4.3.4	Respiratory System	55
Chapter 5: Discussion		56
5.1	Synthesis and Characterization of HPG polymers	56
5.2	In vitro analysis of HPG polymers.....	57
5.3	In vivo analysis: Biodistribution of HPG polymers in mice	61
Chapter 6: Summary and Future Studies.....		64
6.1	Summary	64
6.2	Recommended Future Studies.....	65
Bibliography		67
Appendix.....		78

List of Tables

Table 1: Commonly used PD solutions manufactured by Baxter	6
Table 2: MW, size and PDI values of HPG, HPG+1S and HPG+3S	30
Table 3: Mean K_m values of the polymer candidates in hepatocyte cell lines.	40

List of Figures

Figure 1: Annual health care costs of dialysis stratified by modality in Canada(30).	4
Figure 2: Schematic showing harmful effects of conventional PD solutions that new PD solutions aim to control (36).	7
Figure 3: General Scheme for ring opening multi-branching polymerization of HPG (41).....	9
Figure 4: Ultrafiltration of HPG solutions compared to that of Physioneal solution.(46).....	10
Figure 5: Comparison of Physioneal (PYS), icodextrin (ICO), and HPG in the preservation of peritoneal membrane structure and function(48).	11
Figure 6: Binding model for ASGP-R ligands in an optimal conformation to the heterooligomeric receptor consisting of H1 and H2 subunits (51).	13
Figure 7: A schematic of receptor mediated active targeting of hepatocytes (55).....	13
Figure 8: Conversion of N-acetyl-D-galactosamine to D-galactopyrano-2-oxazoline.	17
Figure 9: Formation of Allyl-GalNAc from Galactopyrano-2-oxazoline using allyl alcohol. 18	
Figure 10: Conversion of allyl-GalNAc to GalNAc epoxide.....	19
Figure 11: Conjugation of HPG with epoxy-GalNAc.....	19
Figure 12: Deprotection of acetyl groups to hydroxyl groups.	20
Figure 13: NMR of HPG 3K.....	31
Figure 14: NMR of HPG 3K with one GalNAc group (HPG+1S)	31
Figure 15: NMR of HPG 3K with three GalNAc groups (HPG+3S)	32
Figure 16: Time dependent internalization of Alexa 647 tagged HPG+3S, HPG+1S, and HPG in three hepatocyte cell lines using flow cytometry. A) In HepG2 cells. B) In HuH7.5.1 cells. C) In THLE2 cells.....	34

Figure 17: Polymer internalization in HepG2 cells fixed using 4%PFA in culture slides. A) Red, HPG; blue, DAPI nuclei staining. B) Red, HPG+1S; blue, DAPI nuclei staining. C) Red, HPG+1S; blue, DAPI nuclei staining. 35

Figure 18: ASGPR1 receptor staining in different human hepatocyte cell lines using flow cytometry. Red: background staining, Blue: ASGPR1 staining. A) HepG2 cells: high expression. B) HuH7.5.1 cells: moderate expression. C) THLE2 cells: low expression..... 36

Figure 19: Determination of affinity of HPG polymer and polymer conjugates using flow cytometry. A) Dose dependent response in HepG2 cells. B) Dose dependent response in HuH7.5.1 cells. C) Dose dependent response in THLE2 cells D) Comparison of K_m values across the hepatocyte cell lines panel..... 39

Figure 20: ASGPR1 receptor staining in HEK293 cells using flow cytometry. Red: background staining, blue: ASGPR1 staining. A) ASGPR^{-/-} B) ASGPR^{+/-} and C) ASGPR^{+/+}. 41

Figure 21: Uptake analysis of HPG and HPG+3S in HEK293 cells using flow cytometry. ASGPR^{-/-}: HEK 293 cells, ASGPR^{+/-}: HEK293 cells expressing ASGPR1 gene, ASGPR^{+/+}: HEK293 cells expressing ASGPR1 and ASGPR2 gene. 42

Figure 22: A) Competitive Inhibition of HPG+3S using flow cytometry in the presence and absence of asialofetuin. B) Percentage inhibition of uptake of HPG+3S by asialofetuin. C) Competitive inhibition of HPG+3S by GalNAc using flow cytometry. 44

Figure 23: Efflux of HPG polymers in HepG2 cells after 2 hours of treatment. 45

Figure 24: Comparison of receptor expression in hepatocytes (HepG2) vs monocytes (THP-1) Red: background staining, blue: ASGPR1 staining. HepG2: High expression, THP-1: low expression..... 46

Figure 25: A) Time dependent uptake of HPG polymers in THP-1 cells. B) Comparison of uptake of HPG polymers in THP-1 and HepG2 cells. 47

Figure 26: Distribution of HPG compared to HPG+3S for 48 hours. A) Percent of injected dose retained in the Liver. B) Percent of injected dose excreted out through feces. 49

Figure 27: Distribution of HPG compared to HPG+3S in organs of the digestive system. A) Percent of injected dose retained in stomach and Gall bladder. B) Percent of injected dose retained in the small and large intestine. 50

Figure 28: Distribution of HPG and HPG+3S in the urinary system. A) Percent of injected dose retained in the Kidney. B) Percent of injected dose excreted via Urine. 52

Figure 29: Distribution of HPG and HPG+3S in the circulatory system. A) Percentage of injected dose retained in the heart. B) Percentage of injected dose retained in the spleen. C) Percentage of injected dose retained in the whole blood and plasma. 54

Figure 30: Percent of injected dose retained in the lungs. 55

List of Symbols

IC_{50} - Inhibitory Constant

K_m - Michaelis-Menten Constant

List of Abbreviations

APC	Allophycocyanin
APD	Automated Peritoneal Dialysis
APTT	Activated Partial Thromboplastin Time
ARF	Acute Renal Failure
ASGPR	Asialoglycoprotein Receptor
BCCRI	BC Cancer Research Institute
CAPD	Continuous Ambulatory Peritoneal Dialysis
CRF	Chronic Renal Failure
CVD	Cardiovascular Disease
DCM	Dichloromethane
DMEM	Dulbecco's Modified Eagle Medium
DMF	Dimethylformamide
EGF	Epidermal Growth Factor
ESRD	End-Stage Renal Disease
FBS	Fetal Bovine Serum
FBS	Fetal Bovine Serum
FITC	Fluorescein Isothiocyanate
FITC	Fluorescein Isothiocyanate
GalNAc	N-acetylgalactosamine
GFR	Glomerular Filtration Rate
GPC	Gel Permeation Chromatography

HD	Hemodialysis
HPG	Hyperbranched Polyglycerol
HPMC	Human Peritoneal Membrane Cells
ICO	Icodextrin
MFI	Mean Fluorescence Intensity
MW	Molecular Weight
NaH	Sodium Hydride
NMR	Nuclear Magnetic Resonance
PBS	Phosphate Buffered Saline
PD	Peritoneal Dialysis
PDI	Polydispersity Index
PEG	Polyethylene glycol
PRT	Plasma Recalcification Time
PYS	Physioneal
RBC	Red blood cell
ROMBP	Ring opening Multi-branching Polymerization
TLC	Thin layer chromatography
TMSOTf	trimethylsilyl triflate
VGH	Vancouver General Hospital
VWF	Von Willebrand Factor

Glossary

IC₅₀ – It is the concentration of inhibitor required to reduce binding of another substance to the receptor by 50%.

K_m – K_m value is an index of the affinity of an enzyme for its substrate. In this case, it refers to the affinity of ASGPR receptor for the various HPG polymers. The lower the K_m value the better the affinity.

Acknowledgements

I extend my sincere thanks to Dr. Caigan Du for taking me as his graduate student and always being approachable. I appreciate the patience he had while answering my never-ending questions and spirals which slowly shaped my thought processes. I would like to thank Ms. Qiunong Guan for her constant moral support and technical guidance. I would like to thank Dr. Jaychandran Kizhakkedathu and his whole team who provided support and helped in the chemistry part of this project. A special thanks to Ms. Irina Chafeeva for letting me shadow her for months, teaching me to set up various reactions and making sure I did everything right. I extend my sincere thanks to Dr. Srinivas Abbina for explaining complicated chemistry to a person with no chemistry background and always believing and encouraging me like a mentor. I would like to thank all the lab members of both the labs. A huge thanks to CIHR and Michael Smith foundations for providing financial support to our research project. I would like to thank Dr. Dirk Lange and his lab for always being welcoming and kind even after I finished my lab rotation. I would like to thank the whole team led by Ms. Nicole Wretham at BCCRI for their support with in vivo experiments.

A special thanks to Sara Khoddami for being a resourceful classmate and sweetest friend for the past 2 years. I would further like to thank all my long-distant buddies (Mythili, Sujitha, Vishnu, and Mani) for the constant moral support and occasional pandemic gaming. I extend my gratitude to all my friends (especially Keren, Varun, Jahnavi, 'Onam group' and roommates) in Vancouver who turned into foster family and helped me maintain a good work-life balance. Their support made going through grad school, divorce, and a pandemic in a foreign country easier.

I thank my Mom, Dad, Brother, Uncles, Aunts, and cousins for all the love and support by all possible means. A special thanks to my dear nephew (Nithil) and my cousin (Mala) for checking on me almost every day ever since I started my application process.

To my grandmother Mrs. Brema Meenatchinathan who played (and still does) an important role in instilling the importance of seeking knowledge at a very young age in me. My master's is a fruit of her constant encouragement to prioritize education over any other desire.

Chapter 1: Introduction

The kidneys are responsible for various bodily functions such as regulating water and mineral levels, removing impurities/waste substances, producing hormones etc. The Urology Care Foundation suggests that the term “Kidney failure” refers to a lot of problems which include improper blood supply to the kidneys, blockage caused by stones, polycystic kidney disease, glomerulonephritis, and nephropathies caused due to hypertension and diabetes (1). Kidney failure can be of two types: Acute Renal Failure (ARF) and Chronic Renal Failure (CRF). ARF is characterized by abrupt increase in creatinine levels that is caused due to an injury or insult that causes a structural or functional change in the kidney. With ARF, renal function can be reverted to normal if the cause is treated (2). CRF is gradual and permanent loss of renal function that goes unnoticed until the kidney function goes as low as 20% (1). CRF will eventually lead to End Stage Renal Disease (ESRD) which is defined as an irreversible loss in renal function that can be fatal without intervention such as dialysis or transplant (3). The prevalence of ESRD is reported to be greater in countries like the US and Japan (4,5). In Canada, the annual overall prevalence for CRF is 12.5% with around 0.73 million people progressing to ESRD according to a study in 2013(6). The number of ESRD patients has been on the rise since 1980 in Canada and is also predicted to keep increasing (7–9). Progression to ESRD is linked to other co-morbid conditions like diabetes, hypertension and cardiovascular disease and accounts for about 16 times more than the average healthcare cost for a person and has serious implications (6,7). The best treatment option for ESRD is kidney transplant followed by dialysis. According to a statistics report on organ replacement, 42% of patients received a transplant kidney in 2017. The remaining 58% received some form of dialysis (10). Patients are put on some sort of dialysis until a donor kidney is found.

1.1 End Stage Renal Disease

Patients with glomerular filtration rate (GFR) of less than 15 mL per 1.73m² body surface area or requiring dialysis irrespective of GFR for survival are identified to have ESRD as per the National Kidney Foundation(3). ESRD can often be called stage V of CRF but differs from CRF by the fact that, in ESRD patients require long-term dialysis for survival (11). ESRD is characterized by fluid retention in the body which in turn leads to hypertension, ventricular dysfunction which further leads to cardiovascular disease (CVD), disruption of bone and mineral metabolism, dyslipidemia and protein energy malnutrition. Anemia is also associated with ESRD due to reduced erythropoietin synthesis by the affected kidneys (3). People aged 65 years and above have a four times greater chance of progressing to ESRD (1). Hypertension and proteinuria are considered two of the strongest factors contributing to quick progression to ESRD. (12,13). There has been a striking increase in percentage of ESRD patients with diabetes as the primary prognosis. In fact, diabetes has progressed to become the number one cause for nephropathies leading to ESRD (13–16). The prognosis of ESRD remains poor and mortality rates are linked to infection during dialysis, CVD, acidosis etc. (3).

1.2 Dialysis

Dialysis is a treatment method which is used to remove impurities or uremic toxins from the body through artificial means. It is of two types: Hemodialysis and Peritoneal Dialysis (PD). Hemodialysis is a method where an artificial kidney or hemodialyzer is used. The blood is usually drawn out from the femoral vein or fistula and passed through an extracorporeal machine with several filters that filter blood and then the purified blood is sent back to the

patient. Hemodialysis aims to restore intracellular and extra cellular chemical/fluid balance that is normally maintained by the kidneys. This is done by the movement of solute particles such as urea, phosphates, albumin and other protein bound solutes across a semi-permeable membrane with the help of hydrostatic or osmotic pressure(17–19). Patients may be required to do dialysis twice per week to daily depending on the extent of residual renal function. Frequency of dialysis is also determined by several factors such as amount of uremic toxins generated, body mass and other clinical conditions (17,20). There are several risk factors associated with hemodialysis such as hypotension, embolus formation, increased risk of CVD due to vascular stiffness and calcification. Sepsis is the second most common cause of death in dialysis patients after cardiovascular related deaths (21–24). Hemodialysis is not the focus of this thesis and hence will not be discussed further.

1.3 Peritoneal Dialysis:

PD is a type of dialysis in which a catheter is implanted in the peritoneum of the patient and a highly osmotic solution is poured into the peritoneum and later drained (known as exchange) (25). There are three different types of PD: Continuous Ambulatory peritoneal dialysis (CAPD), Automated Peritoneal Dialysis (APD) and a combination of both. In APD, an automated cyler is used to perform the exchanges when the patient is sleeping in the night. In CAPD, 4 to 5 exchanges are performed during the day, with the help of gravity and no machine is needed (26). PD also allows patients to continue employment and does not put financial pressure on patients as much as hemodialysis. In 2017, 23% of new patients who started dialysis opted for PD (10). Comparison of dialysis costs throughout the world show that costs incurred for PD is much cheaper than for hemodialysis. In Canada, the average annual costs per patient for hemodialysis (in unit) is estimated to be \$64,214 and for PD is estimated to be

\$38,658 (27). From Figure1, we can see the cost distribution for different types of treatment modalities for renal failure. Although, the material costs for PD are higher than hemodialysis, the total costs for PD is much lesser than hemodialysis. Inclusion of inpatient and outpatient costs, training of personnel, medication, and other hidden costs such as transportation costs and patient productivity suggest PD to be much more advantageous (28–30). Naturally, the question arises why only a small percentage of renal failure patients undergo PD despite the increased cost effectiveness and quality of life. Factors like age, predisposition to other disease such as immune disorders, diabetes, hypertension, abdominal surgeries, and peritoneal membrane health all contribute to the recruitment of patients for PD.

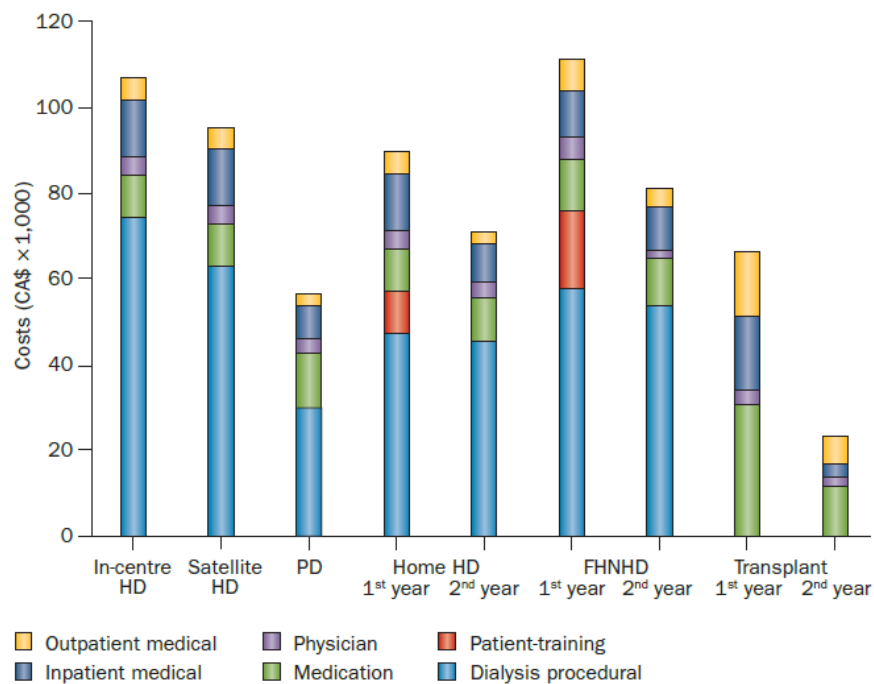


Figure 1: Annual health care costs of dialysis stratified by modality in Canada(30).

The success of PD depends on the ultrafiltration ability of the peritoneal membrane. The peritoneal membrane consists of a monolayer of mesothelial cells underneath which lies a rich network of capillaries. These mesothelial cells are responsible for maintaining peritoneal

homeostasis and this ability is exploited to perform dialysis. The membrane allows solute transport and fluid balance but is prone to inflammation and fibrosis (31). The major drawback with PD is ultrafiltration failure which is normally caused due to fibrosis and infection of the peritoneal membrane (32). Thus, the use of a safe and biocompatible osmotic agent is highly essential. PD solutions are composed of an osmotic agent, buffer, and electrolytes. Glucose is the most common osmotic agent and conventional PD solutions use either glucose or glucose-based polymers. It is known that 39% of new patients with ESRD are diabetic (10).

There is increasing evidence that conventional PD solutions lead to local and systemic toxicities. Glucose degradation products are generated and contribute to lower pH of the dialysis solutions. Icodextrin, a poly-glucose solution was used. Icodextrin solutions are isosmotic and have low ultrafiltration rates hence used for long dwell times. Amino acid-based PD solutions contain 1.1% amino acids which have similar osmolarity rates to 1.5% dextrose solutions but are associated with acidosis and raise in urea/ nitrogen levels. Neutral pH solutions comprised of 2 or more bags that must be mixed before use were introduced. More data on the use of these neutral pH PD solutions are needed. The use of conventional PD solutions is still required despite the newer PD solutions because none of them completely replace glucose-based PD solutions and only aim to reduce the use of conventional PD solutions in hopes of prolonging PD treatment. Use of conventional PD solutions is associated with loss of mesothelial layer, inflammation, angiogenesis with vasculopathy and fibrosis locally. Systemic effects include hyperglycemia, dyslipidemia, oxidative stress and metabolic syndrome, endothelial dysfunction and decrease in residual renal function. These effects eventually lead to cardiovascular diseases(25,31,33–36).

Table 1: Commonly used PD solutions manufactured by Baxter.

Solution	pH	Osmotic Agent	Level of GDP	Disadvantages
Dianeal	5.2	Glucose (5-42.5g/L)	High	Low pH; damages peritoneal membrane; systemic glucose exposure; infusion pain
Physioneal (Two chamber)	7.4	Glucose (15-42.5g/L)	High	Local and systemic damage due to glucose exposure
Extraneal	5.6	Icodextrin (75g/L)	Low	low pH; hypersensitivity; single daily use; longer dwell times
Nutrineal	5.5	Amino Acids (1.1% solution)	No	Acidosis; single daily use; low pH

With more patients being diabetic, there is a need for non-glucose based peritoneal dialysis solution that is safer for the peritoneal membrane, limits the systemic effects of glucose and enables diabetes induced nephropathic patients to opt for PD. For this, a small biocompatible osmotic agent that will not elicit an immune response and that can impart high osmolarity to PD solutions will be ideal.

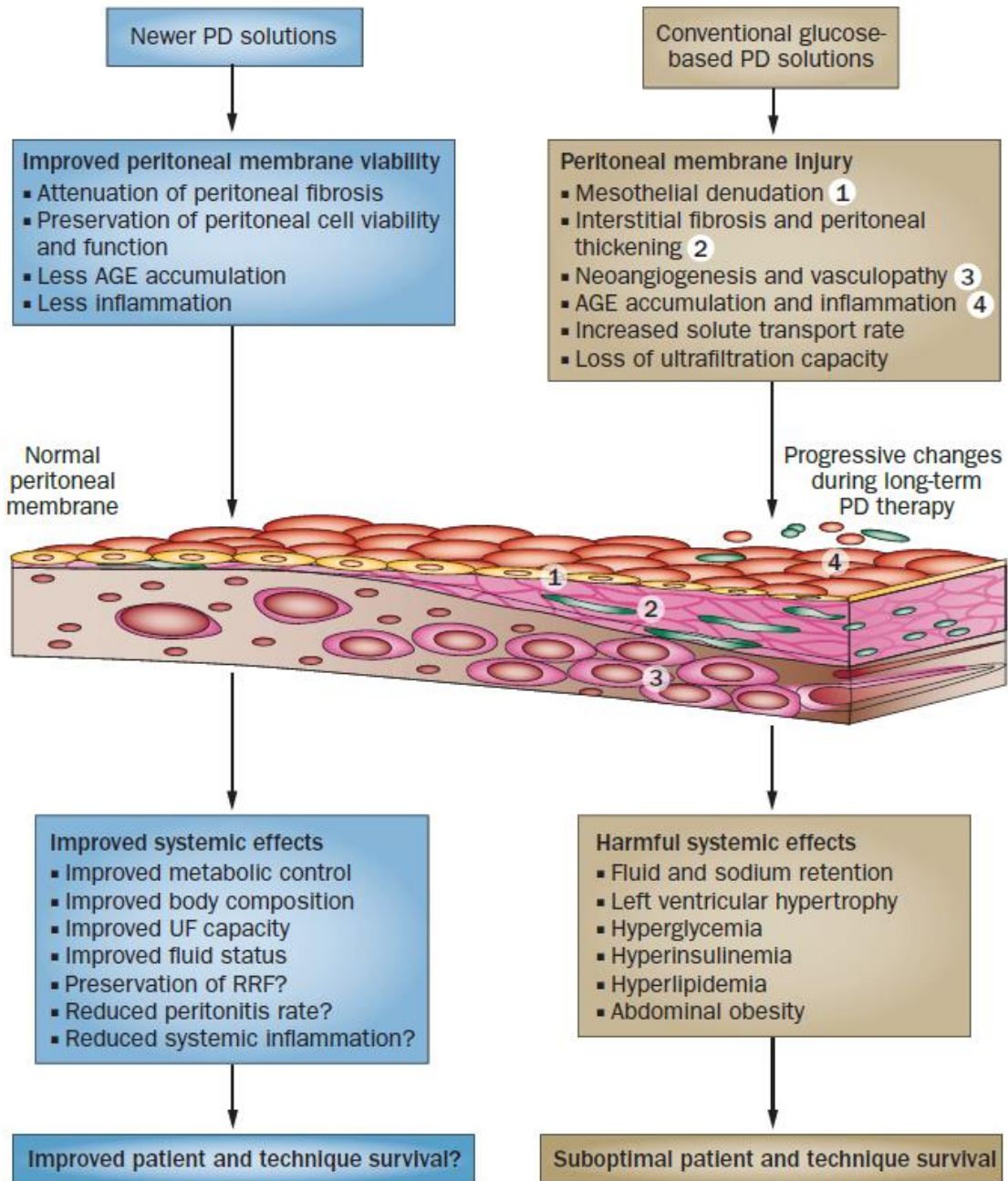


Figure 2: Schematic showing harmful effects of conventional PD solutions that new PD solutions aim to control (36).

1.4 Hyperbranched Polyglycerol (HPG):

In 1999, a group of scientists from Germany showed that hyperbranched polyglycerol (HPG) can be synthesized using glycidol monomer (AB₂ latent cyclic monomer) by ring opening multi-branching polymerization (ROMBP) reactions. Through controlled and slow monomer addition, hyperbranched dendritic polyglycerols with polydispersity less than 1.5 can be synthesized (37). Glycerol being found in phospholipids, the newly found polymer was expected to be biocompatible and used for biomedical applications. In one of the earliest reviews of HPG by Holger Frey and Ranier Haag list several applications. HPG will make good hydrogels owing to the dendrimers present. The OH groups can be modified with cell growth factors that can stimulate cell growth and provide a scaffold. Esterification with fatty acids created an amphiphilic core which enables use as nano capsules and nano particles that can be used as topical ointments and in drug delivery(38,39).

HPG has a very similar structure to polyethylene glycol (PEG) and is very biocompatible. In 2006, biocompatibility testing on both linear and hyperbranched polyglycerols of lower molecular weight showed no significant complement activation or red blood cell (RBC) aggregation and hence was deemed biocompatible and hemocompatible(40). Both in vitro and in vivo biological evaluations of higher molecular weight HPGs (100 K – 800 K) show that HPG is more thermally stable than PEG and behaves protein-like in a solution. HPG does not elicit any immunological responses when injected in mice and rats. It is actively flushed out of the system by the kidneys although the higher molecular weight HPG take more time for clearance (41,42).

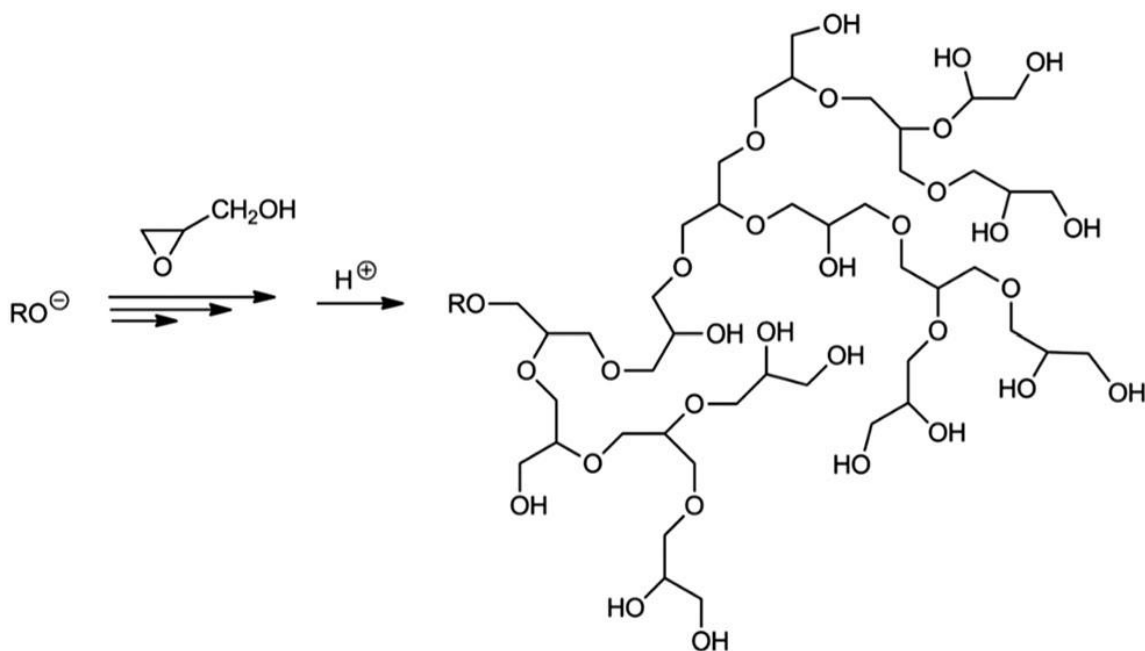


Figure 3: General Scheme for ring opening multi-branching polymerization of HPG (43).

A decade of research in HPG extends in various directions such as regenerative medicine, colloidal organ preservative, theranostic applications, drug delivery, polymer therapeutics and imaging applications (43,44). In 2007, Brooks and colleagues first demonstrated the use of HPG as an osmotic agent by the development of an improved low viscosity substitute for human serum albumin (45). Later in 2013, Sprague Dawley rats (10-12 weeks old) were given peritoneal injections of solutions containing low molecular weight HPG as the osmotic agent and compared with the conventional physioneal solution. HPG solutions showed good ultrafiltration properties with efficiency increasing with increase in molecular weight of the polymer (46).

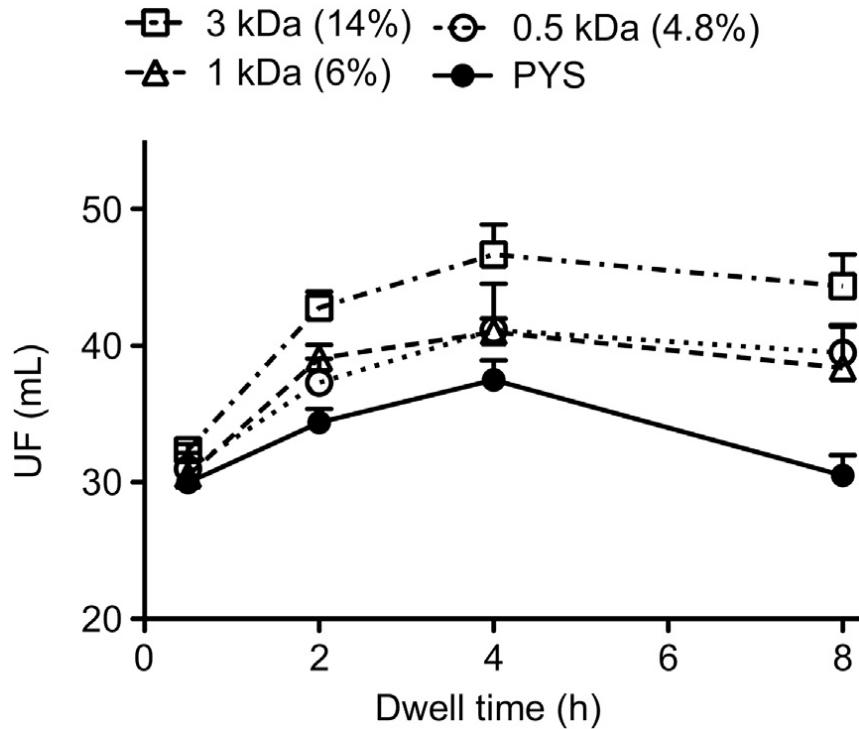


Figure 4: Ultrafiltration of HPG solutions compared to that of Physioneal solution.(46)

HPG solutions not only show good ultrafiltration, but also cause less damage to the peritoneal membrane than conventional physioneal solution. It is also to be kept in mind that the physioneal solution is the better solution among conventional dialysis solution. Moreover, in cultured human peritoneal mesothelial cells (HPMC), HPG solutions were found to induce apoptosis versus necrosis by conventional PD solutions. Further research on the local and systemic effects of HPG versus conventional solutions for a long term (3 months) in rats show that the physioneal solution triggered more inflammatory cytokine production than HPG solution (46,47). When obese diabetic rats received Physioneal, icodextrin and HPG (1K) solutions, HPG solution shows better ultrafiltration and less peritoneal membrane damage and lesser changes to blood metabolic panel and cytokine profile(48).

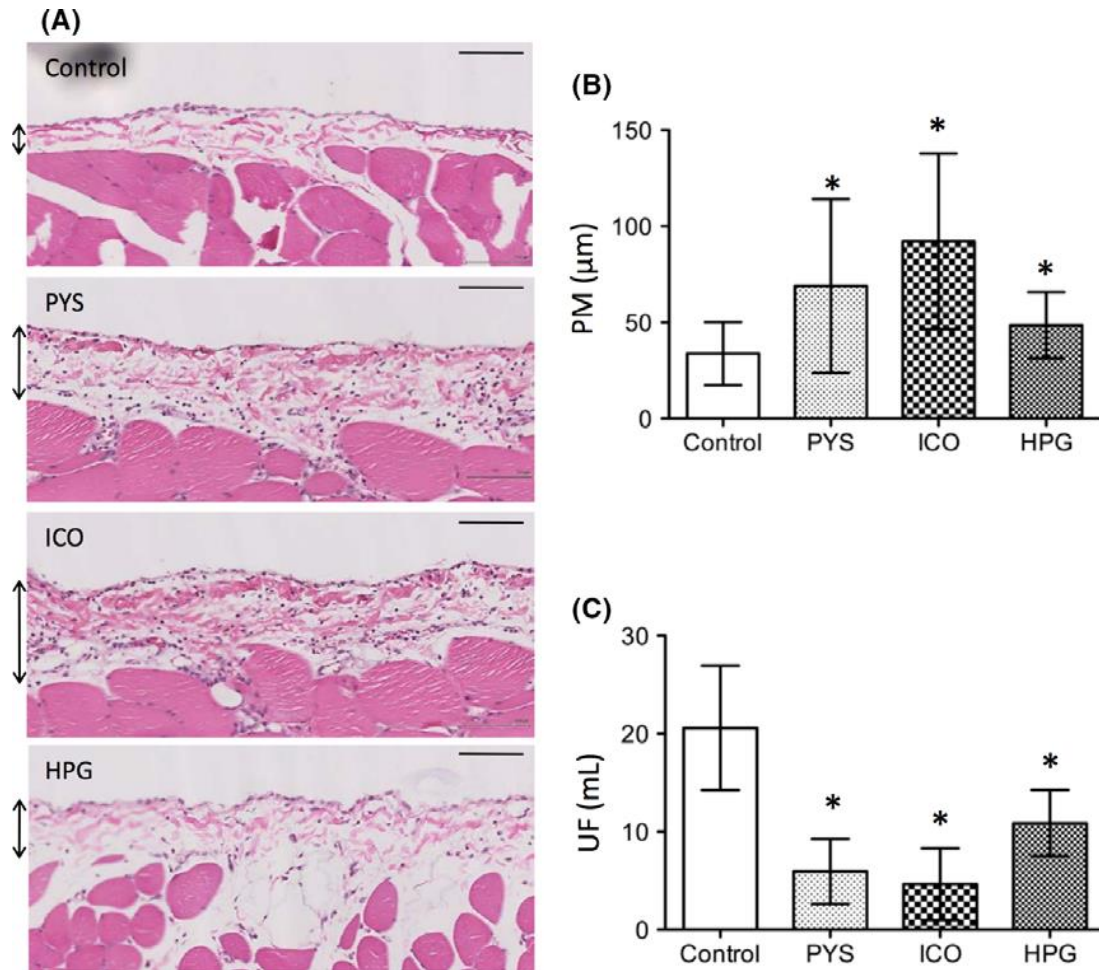


Figure 5: Comparison of Physioneal (PYS), icodextrin (ICO), and HPG in the preservation of peritoneal membrane structure and function(48).

Although, HPG polymers show good ultrafiltration properties and better preservation of the peritoneal membrane, our group has found out that HPG excretion is mainly dependent on kidney function (data not published yet). Since, we are considering HPG for dialysis solutions for a long term, we need to keep in mind that PD patients have reduced residual renal function and the goal of PD is to preserve this function. HPG accumulation in the long run may turn into a health hazard for prolonged use of HPG based PD solutions. Thus, there is a need to find a by-pass route for HPG that might be absorbed by the body during exchanges to be excreted. Liver targeting and biliary excretion is one way of creating a by-pass route and can

be achieved by aiming to target the ASGPR which is a receptor found predominantly in hepatocytes.

1.5 Asialoglycoprotein Receptor (ASGPR):

The asialoglycoprotein receptor (ASGPR) also known as the Ashwell-Morell receptor is one of the first C-type lectin receptors to be discovered. It is known to be expressed in the parenchymal cells of the liver (sinusoidal surface) predominantly. It is also found to be expressed in monocytes, peritoneal macrophages, testes, human sperm, and epithelial cells of the intestine. (37). ASGPR plays a role in regulating the number of glycoproteins in the blood by identifying proteins that are highly glycosylated at the terminal galactose and GalNAc residues. Upon ligand binding, ASGPR is internalized by clatherin mediated endocytosis and then receptor-ligand complexes are broken down with the help of lysosomes. Ligand binding and internalization is dependent on Ca^{2+} ions (49,50).

The receptor is a complex transmembrane hetero-oligomeric structure consisting of two types of polypeptide chains H1 and H2 encoded by ASGPR1 and ASGPR2 genes, respectively. The receptor is formed by assembly of these chains in a 2:1 ratio (51). There is a total of 5 isoforms of the ASGPR: 2 isoforms of ASGPR1 gene (1a and 1b) and 3 isoforms of ASGPR2 gene (2a,2b and 2c). The amino acids aspartic acid 241, aspartic acid 265, asparagine 264, glutamic acid 252, glutamine 239 and tryptophan 243 belonging to H1 are recognized to be the active site for ligand binding. A glycine rich loop protrudes from the surface to which sugars are attracted to the binding pocket where the second calcium ion binds to the sugar (52).GalNAc residues have been found to bind more tightly than galactose residues (49,53).

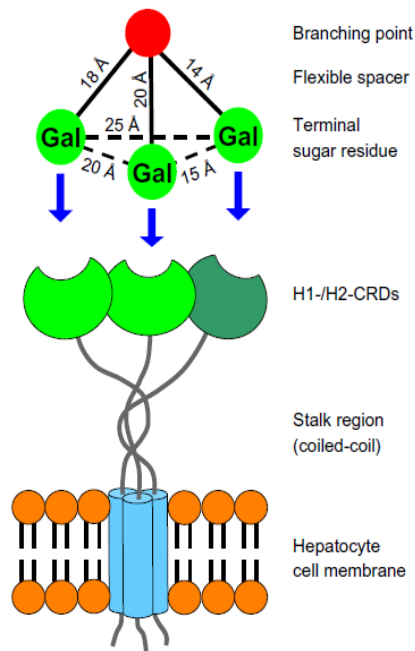


Figure 6: Binding model for ASGP-R ligands in an optimal conformation to the heterooligomeric receptor consisting of H1 and H2 subunits (54).

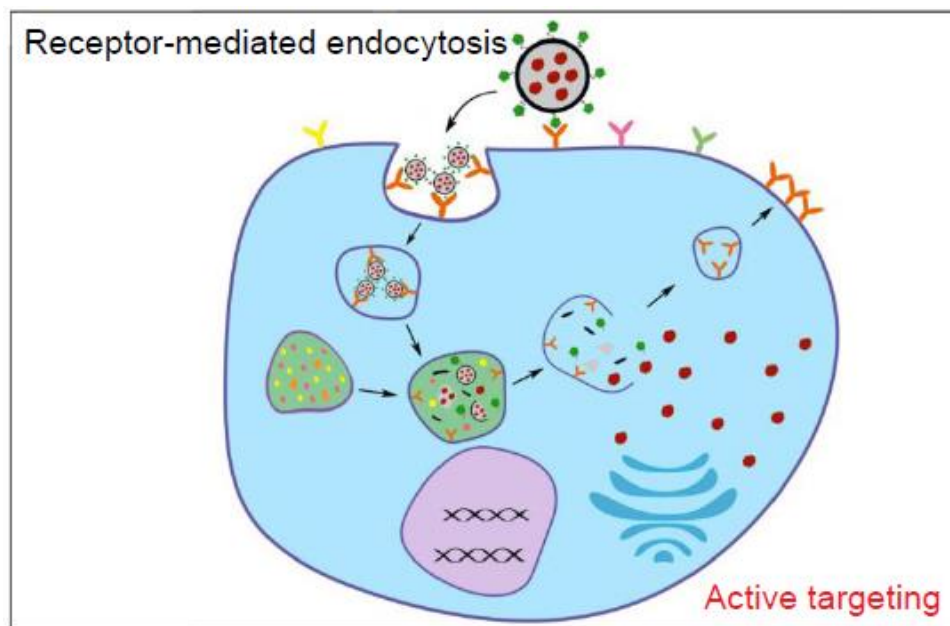


Figure 7: A schematic of receptor mediated active targeting of hepatocytes (55).

The presence of the ASGPR in hepatocytes in large numbers proved to be an effective liver targeting strategy. By conjugating galactose or GalNAc to liposomes, micelles, or dendrimers successful receptor mediated uptake by hepatocytes have been achieved(49). An increase in the number of GalNAc moieties presents increased uptake and stronger binding ability to the receptor. Several groups have come up with this strategy to selectively target the liver especially for drug delivery for hepatocellular carcinoma(49,54–57). Preclinical gene therapies with GalNAc conjugated siRNAs have shown to successfully target hepatocytes (58–60). Revirusan, a GalNAc-siRNA conjugate targeting transthyretin in for treatment of transthyretin mediated amyloidosis emerged successful in clinical trials (61).

Chapter 2: Objective of the thesis

From literature review, we know that there is a consistent increase in the incidence of ESRD patients with primary prognosis of diabetes. Amongst the very few treatment options available to them, they are not able to opt for peritoneal dialysis due to the use of glucose as the main osmotic agent. Albeit HPG shows promising ultrafiltration and lesser peritoneal membrane damage than glucose-based solutions, it still poses the risk of accumulating within the body since HPG is primarily excreted via the kidneys. On the other hand, ASGPR mediated liver targeting is a well-researched method for targeted delivery of drugs and gene therapies to hepatocytes and has emerged successful over these recent years.

We hypothesize that conjugation of HPG with GalNAc will generate a non-glucose osmotic agent with liver targeting capability, thereby providing a new elimination route via feces for HPG and ameliorate the pressure on the failing kidneys in CRF and ESRD patients who opt for PD. This will excavate PD as a safe renal replacement therapy option for diabetic CRF and ESRD patients which could in turn help in the reduction of health care costs for the government.

With the intention to prove our hypothesis, we have the following specific aims:

1. The first is to successfully conjugate low molecular weight HPG to GalNAc. We decided to synthesize a few polymer conjugates with different number of GalNAc per HPG. Therefore, synthesis of HPG-GalNAc conjugates is the first step in our project.
2. The next step was to test the binding and uptake ability of HPG-GalNAc conjugates in a panel of hepatocyte cell lines to identify the best performing HPG-GalNAc conjugate.
3. The final step of this thesis is to radiolabel HPG and best performing HPG-GalNAc conjugate and understand its biodistribution and excretion in mice.

Chapter 3: Materials and Methods

This chapter lays out the various materials and methods used in the synthesis of HPG-GalNAc followed by the procedures adopted in vitro and in vivo experiments to analyze polymer conjugates.

3.1 HPG-GalNAc Synthesis

HPG-GalNAc synthesis comprised of four different steps. The first three steps involved the synthesis of the sugar to GalNAc-epoxide. The fourth step comprised conjugation of previously synthesized HPG polymer (3k) to the GalNAc-epoxide. 1,2-dichloroethane, trimethylsilyl triflate (TMSOTf), dichloromethane (DCM), dimethylformamide (DMF) and methanol were the solvents used and were purchased from Sigma Aldrich, Canada. Other materials such as 4A molecular sieves, magnesium sulphate, sodium bicarbonate, meta-chloroperoxybenzoic acid and sodium hydride were all purchased from Sigma Aldrich, Canada as well. All chemical structures were drawn using Chemdraw software.

3.1.1 Step 1: Synthesis of Galactopyrano-2-oxazoline

D-galactopyrano-2-oxazoline was obtained from N-acetyl-D-galactosamine (crude GalNAc) (Biosynth Carbosynth, San Deigo, CA) by using trimethylsilyl triflate (TMSOTf) at 50°C with 1,2-dichloroethane as the solvent.

GalNAc (10 g) was dissolved in 160 mL of anhydrous 1,2-dichloroethane along with 4Å molecular sieves in a sealed reaction vessel under argon atmosphere. TMSOTf (7.5mL) was added to the reaction mixture and left undisturbed overnight. The reaction mixture was then filtered through celite, washed twice with 10% sodium bicarbonate (2 x 50 mL) and thrice with

water (3 x 50 mL). The organic layer was dried over anhydrous magnesium sulphate, filtered, and concentrated under vacuum to obtain a dark brown solid that weighed approximately 6.3g. (yield- 63%) (62). Conversion of GalNAc to D- galactopyrano-2-oxazoline was confirmed by H NMR with the disappearance of the doublet at 7.89 to 7.92 ppm corresponding to proton from NH-CO-CH₂ group (refer to appendix).

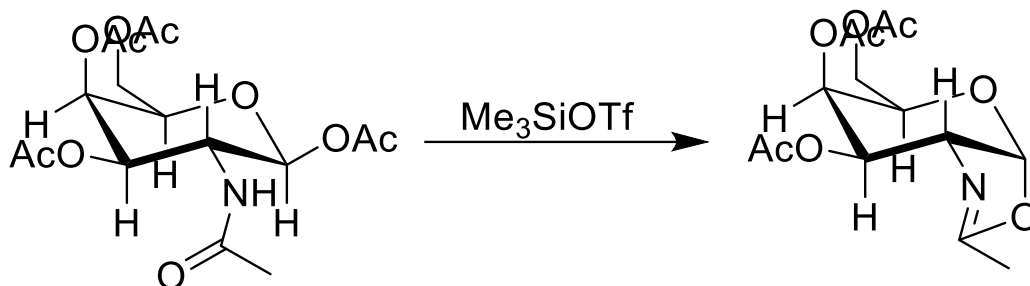


Figure 8: Conversion of N-acetyl-D-galactosamine to D-galactopyrano-2-oxazoline.

3.1.2 Step 2: Gal-2-oxazoline to Allyl-GalNAc

Gal-2-oxazoline obtained from the first step was dissolved in 200 mL of anhydrous 1,2-dichloroethane followed by the dropwise addition of allyl alcohol (14mL) with 4Å molecular sieves under argon atmosphere. The reaction mixture was brought to 70°C and then TMSOTf (1.6 mL) was added. After 20 hours, the reaction mixture was brought to room temperature and filtered through celite. The organic layer was washed first with a saturated solution of sodium bicarbonate (50 mL) twice and then with brine (2 x 50 mL). The organic layer was dried over anhydrous magnesium sulphate, filtered, and concentrated under vacuum to remove excess of allyl alcohol and a colorless white solid was obtained which weighed approximately 5.64 g (yield 89%). The final white solid product obtained would be allyl-GalNAc(62). This intermediary product was verified by H NMR (Nuclear Magnetic Resonance) with the

reappearance of the doublet at 7.89-7.92 ppm and the presence of dddd peaks corresponding to protons of the allyl group at 5.84 ppm (refer to appendix).

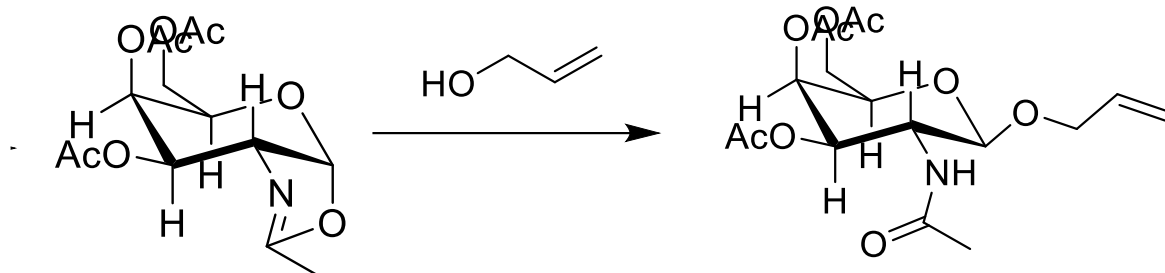


Figure 9: Formation of Allyl-GalNac from Galactopyrano-2-oxazoline using allyl alcohol.

3.1.3 Step 3: Allyl-GalNac to GalNac-epoxide

The allyl-GalNac produced at the end of step 2 was dissolved in 120 mL of dichloromethane (DCM) to which meta chloroperoxybenzoic acid (5.9 g) was added and the reaction mixture was stirred for 24 hours at room temperature. The completion of this reaction was monitored by thin layer chromatography (TLC). A white precipitate, m-chlorobenzoic acid was obtained as a by-product and the reaction mixture was filtered to remove it. The volume of the filtrate was then reduced by 30% with the help of a rotary evaporation and then cooled to 0°C to precipitate more m-chlorobenzoic acid. The concentration-precipitation-filtration cycles were repeated thrice to obtain a white solid of GalNac-epoxide with trace amounts of m-chlorobenzoic acid (62). The final product of sugar modification was confirmed by the presence of characteristic peaks of epoxide at 2.55, 2.70, and 3.06 ppm (refer to appendix).

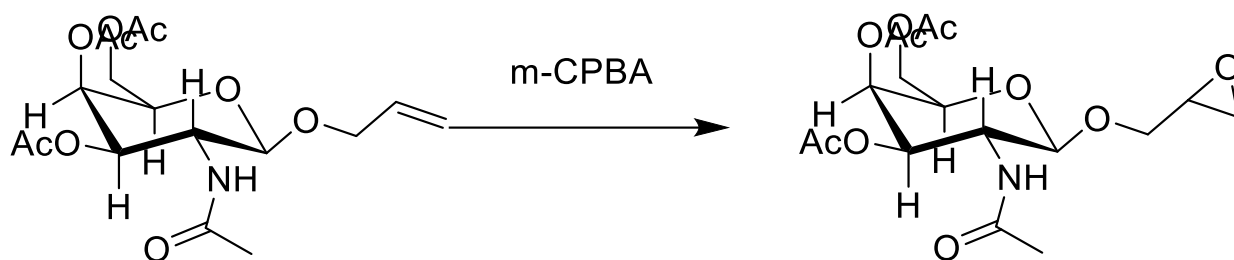


Figure 10: Conversion of allyl-GalNAc to GalNAc epoxide.

3.1.4 Step 4: Conjugation of HPG-3K with GalNAc-epoxide

To the solution of HPG 3K in anhydrous dimethylfluoride (DMF) (100 mL), sodium hydride (approximately 20 mg) was added under argon atmosphere. The reaction mixture was stirred for 2 hours at 70°C and then a solution of GalNAc-epoxide in anhydrous DMF was added to it dropwise (with the help of an injection pump) and the reaction was continued overnight. The ratio of GalNAc-epoxide and HPG 3K determines the number of GalNAc groups that will be conjugated to HPG 3K and it was varied accordingly to obtain polymers with an average number of one and three GalNAc groups per HPG 3K molecule.

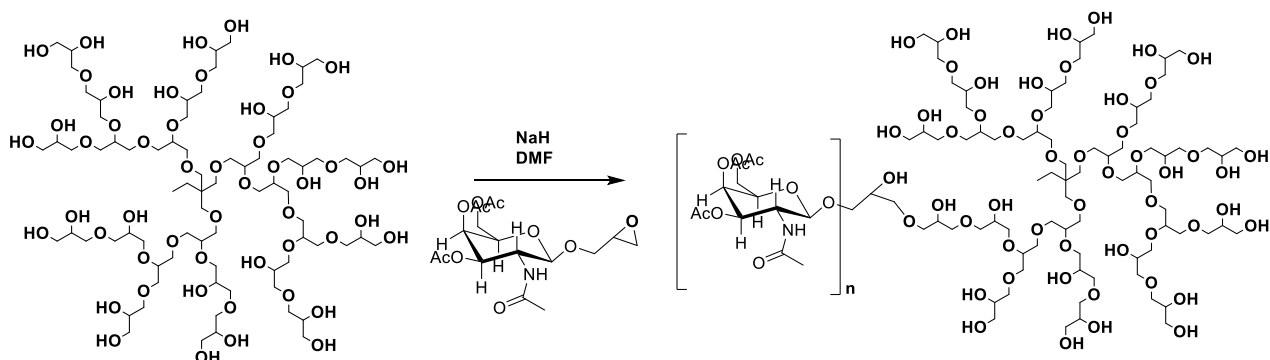


Figure 11: Conjugation of HPG with epoxy-GalNAc.

DMF was removed under reduced pressure and the resulting polymer was then dissolved in anhydrous methanol. Deprotection of the acetyl groups of GalNAc was accomplished by incubating the polymer with sodium methanolate at room temperature for 2 hours initially. After, full conversion was confirmed by presence of characteristic peak corresponding to GalNAc at 2.0 ppm, methanol was removed under reduced pressure and the polymer was dissolved in water, and its pH was adjusted to 7.0 with HCl.

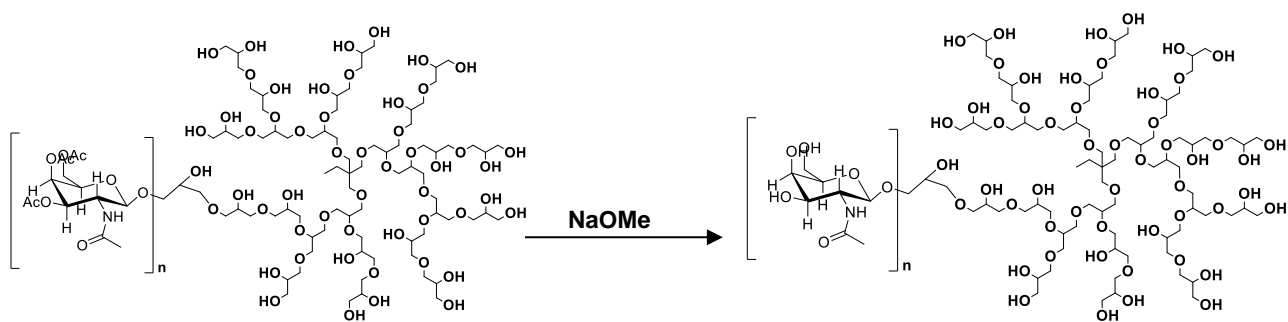


Figure 12: Deprotection of acetyl groups to hydroxyl groups.

The polymer conjugates were characterized using NMR. The products of each reaction were verified using ¹H NMR. Samples were prepared in D₂O or DMSO at each stage of the synthesis and analyzed. The final polymer samples were also run through Gel Permeation Chromatography (GPC) to obtain the size, molecular weight, and polydispersity data (63).

3.2 Labelling of polymer conjugates

There are two methods to label HPG polymer and HPG polymer conjugates: fluorescent dye labeling and radiolabeling. For in vitro studies, Alexa 647 dye which has excitation wavelength of 650 nm and emission at 665 nm and can be detected with the Allophycocyanin (APC) channel was chosen. For in vivo studies, radiolabeling with tritium (³H₁) was chosen.

3.2.1 Alexa 647 labelling

Freeze dried polymer was dissolved in 0.1M sodium bicarbonate buffer (1 mL). Alexa 647 dye (purchased from Thermofisher Scientific, Canada) was dissolved in anhydrous DMF (5 mg in 0.5 mL). 75-80 μ L of dye solution was added to the reaction mixture and continuously stirred at room temperature overnight in dark conditions (64). After stopping the reaction, the dye tagged polymer solution was dialyzed in a 1K membrane for 24 hours to remove excess dye, DMF and salts. A much smaller cut-off membrane was used to prevent loss of dye tagged polymer (molecular weight approximately 3K). Dye tagged polymer was then freeze dried and then dissolved in distilled H₂O to make stock solution of 1 mg/mL concentrations.

3.2.2 Radiolabeling

HPG 3K and GalNAc conjugated HPG 3K (HPG+3S) were radiolabeled with tritium (³H₁) for performing in vivo bio -distribution experiments. The radiolabeling reactions were set up using previously established protocols by Irina Chafeeva at the hot lab in Dr.Jayachandran Kizhakkedathu's lab (42,65). The final injectable solutions were then transported to BC Cancer Research facility (Vancouver, BC).

3.3 In vitro: Cell Culture

The panel of hepatocytes chosen for initial screening of the best HPG polymer conjugate included HepG2, HuH 7.5.1 and THLE2 cells.

HepG2 cells provide a good 2D model for liver toxicity and uptake studies. It was derived from a 15-year white male with hepatocellular carcinoma(66). The cells are adherent and epithelial

cell like. HepG2 cells were available in the lab inventory at Dr. Caigan Du's lab. HepG2 cells were cultured in uncoated culture plates with DMEM supplemented by 10% FBS and 1% antibiotics. HuH 7 cells are known for virology research such as the Hepatitis C and dengue virus. They are hepatocellular carcinoma cells derived from a Japanese male in his late fifties (67). HuH 7.5.1 cells were acquired from Dr. Jean Francois laboratory by signing an Material Transfer Agreement with Apath,L.L.C . HuH 7.5.1 cells were cultured similar to HepG2 cells. THLE 2 cells are transformed human liver epithelial cells from an adult male using simian virus 40 (SV40)(68). THLE2 cells were purchased from the American Type Culture Collection (ATCC) and cultured in lab optimized KI^{+/+} media. KI media is prepared by mixing a 1:1 ratio of DMEM and F-12 media along with 1% HEPES modification solution, 0.25% EGF (Epidermal Growth Factor), 10% fetal bovine serum (FBS) and 1% antibiotics. HEK293 cells were cultured using DMEM supplemented by 10% FBS and 1% antibiotics. THP-1 cells were cultured with RPMI media along with 10% FBS and 1% antibiotics.

3.3.1 Initial screening of polymer conjugate internalization in different hepatocytes

Time dependent uptake experiments were performed to get information on the shortest period required for the uptake as well as the time at which the maximum uptake can be seen. This experiment helped in optimization of the time required for treating cells with polymer solutions.

Cells were plated in a 24 well plate with a seeding density of 1×10^5 cells per well and left undisturbed overnight at 37°C. Cells were treated with 2 μ M of polymer solutions (HPG, HPG+1S, HPG+3S) in their respective media including the presence of FBS and incubated for different time points starting from 30 minutes up to 4 hours. Previous studies had used

concentrations ranging from 0.4 to 12.5 μM . A concentration that would be ample for the cells yet not saturate them very soon was chosen. Initially, it was planned to check the uptake up to 24 hours but since more than 90% of cells were positive at 4 hours, time points till 4 hours were opted(54,57,69). After incubation, the supernatant was collected, and the cells were washed with phosphate buffered saline (PBS), collected in tubes, centrifuged at 5000rpm for 5 minutes and resuspended in PBS. The cells were analyzed using BD-FACS canto using the APC channel (650 nm-785 nm) and Flowjo software.

For visualization of the internalization of the polymer in cells, HepG2 cells were seeded in single chambered glass slides with a seeding density of 2×10^5 cells and left undisturbed overnight. Cells were treated with 2 μM of polymer solutions and incubated for 1 hour. Media was discarded and cells were washed with PBS. 4% paraformaldehyde was used to fix cells and nuclei were stained with DAPI dye. Chambers were removed and cells were mounted. Cells were imaged using Z stack feature in a confocal microscope (ZEISS LSM 900).

3.3.2 Receptor Mediated Internalization

After confirmation of internalization of the polymers, it was necessary to confirm receptor mediated uptake. To prove this, the following experiments were performed:

1. Confirmation of expression of the ASGPR in hepatocyte cell lines.
2. Dose dependent uptake to determine the K_m values of different polymers.
3. Uptake in the cells ectopically expressing ASGPR.
4. Inhibition assays with natural ligands.

3.3.2.1 ASGPR expression in the panel of hepatocyte cultures

Panel of hepatocytes were stained for presence of ASGPR to know the amount of ASGPR expressed in each cell line which was helpful in correlation of the difference in the uptake observed amongst the cell lines during initial internalization screening and aided in choosing the optimal cell line as a 2D model.

Cells were collected in tubes and washed with 1% FBS solutions and then incubated with primary antibody-ASGPR1(Santa Cruz Biotech) for 30 minutes on ice protected from light. Cells were then washed twice with 1% FBS and incubated with secondary antibody that was tagged with a fluorescent label (FITC). Unstained cells were used as a background control. Both the cells were run through a flow cytometer and analyzed using the FITC channel (490 nm-520 nm, green).

3.3.2.2 Determination of affinity of the polymer conjugates

The goal of this experiment was to determine the Michaelis Menten constant, K_m , of the polymer conjugates to the cell surface receptor. K_m is defined as the concentration at which half of the active sites are occupied and the rate of the reaction is half its maximal value. Hence, the lower the K_m value, the better the affinity of the polymer conjugate to the receptor. This constant was used to determine the polymer conjugate with higher affinity in our experiments. Under ideal conditions, the rate of internalization is used determine K_m values but since it is difficult to determine the rate of internalization, the difference in Mean fluorescence intensities (MFI) was used to arbitrarily determine K_m values. This approach has been adopted from previous studies (57). The Michaelis Menten curve also indicates receptor mediated uptake as binding of a ligand to the receptor is similar to enzyme kinetics.

To determine the K_m values of all the HPG polymer and polymer conjugates, dose dependent uptake was performed by keeping time constant. Cells were seeded in 24 well plate with a seeding density of 1×10^5 per well and treated with different doses of polymer solutions starting from 20 μM and serially diluted till zero. After two hours, the supernatant was collected, cells were collected post two washes with PBS and analyzed using a flow cytometer under the APC channel. With the obtained MFI values, K_m values were calculated through non-linear regression analysis using the Graphpad Prism software. K_m values for each sample was then group analyzed to determine the better performing polymer conjugate. Henceforth, only the better performing polymer conjugate and HepG2 cells were used to save time and resources.

3.3.2.3 Internalization by HEK293 Cells Ectopically Expressing ASGPR

ASGPR predominantly binds GalNAc residues but can bind other sugars as well. Similarly, there would be several other receptors that are capable of binding to our polymer. Hence, it was necessary to confirm that the polymer conjugate internalization is mediated through ASGPR. HEK293 cells are human kidney embryonic cells and naturally do not express ASGPR. An uptake assay using HEK293 cells with and without the receptor genes enabled us to prove that our polymer conjugate is specific to the ASGPR.

HEK293 cells were available from the lab inventory. HEK293 cells expressing ASGPR1 and ASGPR1&2 genes were acquired from Dr. Michael Tanowitz's laboratory at IONIS Pharmaceuticals, California. Cells were cultured in DMEM with 10% FBS. Hygromycin was used to select ASGPR1 positive cells and a mixture of hygromycin and

puromycin was used to positively select HEK293 cells expressing both ASGPR1 and ASGPR2 genes. Cells were seeded in 24 well plate overnight and then treated with 2 μ M solution of HPG and HPG+3S for 2 hours. After incubation, cells were washed with PBS, collected, and analyzed using a flow cytometer using APC channel.

3.3.2.4 Competitive Inhibition of HPG+3S with Natural Ligands

Asialofetuin is a glycoprotein with three asparagine-linked tri-antennary complex carbohydrate chains and terminal N-acetylgalactosamine residues and shows affinity to the ASGPR (54,70). Asialofetuin is used as a natural ligand. The tri-antennary structure of asialofetuin makes it an ideal molecule to perform competitive inhibition studies as our test polymer also has three sugar moieties. Additionally, we used crude GalNAc as well for inhibition studies. The IC₅₀ values of both Asialofetuin (~45.6 μ M) and GalNAc (~4.55mM) is drastically different and hence both were used in experiments to roughly estimate where our polymer conjugate would fall on the affinity spectrum for the receptor(54).

Cells were seeded in 24 well plates with a seeding density of 1 x 10⁵/well and left overnight. Cells were grouped into 3 with one group being the blank, the second group was treated only with HPG+3S (0-2 μ M) for 2 hours and the third group of cells were treated with 8 μ M of asialofetuin in media for 1 hour and then treated with HPG+3S (0-2 μ M) for 2 hours. The cells were then washed with PBS and then run through a flow cytometer. Using the MFI values of group 2 and group 3, percentage inhibition and dose response curves were drawn using the Graphpad Prism. The K_m values of HPG+3S with and without asialofetuin was calculated. For inhibition with GalNAc, cells were pretreated with 10000-fold higher

concentrations of GalNAc and then with HPG+3S. The MFI values were then compared to the cells without the pretreatment, and the percentage inhibition was calculated.

3.3.3 Efflux of HPG+3S from Hepatocytes

HPG+3S internalization through the receptor does not guarantee its breakdown or metabolism. To understand whether HPG+3S is metabolized is very tricky because there are a number of ways in which HPG+3S polymer can be cleaved by the lysosomes. The presence of HPG+3S in the media after washing would indicate that hepatocytes are able to efflux the polymer out from the cell. After treating cells with HPG and HPG+3S (2 μ M) for 2 hours, cells were washed thoroughly with PBS and then switched to fresh media. A volume of 50 μ L from the media was collected and the presence of HPG polymers was tested with the help of a fluorescence spectrophotometer. Due to the sensitivity of the spectrometer being in the microgram level, it was not easy to detect presence of HPG polymers in the media. Hence, an indirect approach employing the flow cytometer was used to see a drop in the MFI values.

HepG2 Cells were treated with 2 μ M of HPG and HPG+3S for 2 hours and then washed thoroughly and incubated with fresh media. Cells were collected at different time points starting with zero hour and ending at 48 hours (0, 2, 4, 24, 48 hours) and run through the flow cytometer and MFI values were recorded and analyzed using Flowjo software.

3.3.4 Internalization of the conjugate in other cells expressing ASGPR.

ASGPR has been found to be expressed not only by the hepatocytes but also by monocytes. THP-1 cells are a good working model and were procured from liquid nitrogen of

the lab inventory. These suspension cells were cultured with RPMI media from Gibco, Thermofisher along with 10% FBS and 1% antibiotics.

Cells were treated with 2 μ M of HPG and HPG+3S for different times starting from 30 minutes up to 4 hours and analyzed with the help of a flow cytometer. The MFI values obtained were also compared to that of the values obtained from HepG2 cells as well.

3.4 In vivo – Bio Distribution of HPG and HPG+3S in C57Bl/6 mice

Radiolabeled HPG and HPG+3S were used for in vivo experiments. All animal experiments with radioactive polymer were performed with the help of the Investigational Drug Program team (led by Dr. Nancy Dos Santos) at the animal facility of BC Cancer Research Institute (BCCRI), VGH campus. The radioactive polymer test solutions were prepared to be injectable at CBR, UBC campus and transported to BCCRI.

Female C57BL/6 mice that were 7-8 weeks old and weighing 17-20g were injected intravenously with a dose of 10 mg/kg. The mice were sacrificed at 2, 8, 24 and 48 hours after injection and their blood, liver, stomach, gall bladder, intestines, heart, lungs, spleen and kidneys were collected. Urine and feces were also collected to examine the percent of polymer excreted. The radioactivity in the tissue and excreta were recorded with the help of a scintillation counter. The radioactivity present in each tissue was used to calculate the percent of polymer retained in tissue by dividing it with the radioactive count of the polymer injected to each mouse.

3.5 Statistical analysis

Graphpad prism 8.0 software was used to analyze graphical data. For multiple comparisons two-way ANOVA was used. For comparing means between two groups two-tailed unpaired Student t-tests were used.

Chapter 4: Results

4.1 Characterization of HPG polymers

NMR (nuclear magnetic resonance spectroscopy) analysis of the three polymers were done by dissolving about 10 mg of the polymer in approximately 1 mL of D₂O. NMR analysis helps to determine the molecular structure of the HPG-GalNAc conjugates. In this case, NMR analysis was done to estimate the number of sugar moieties present in HPG 3K polymers. The molecular weight (MW), size and polydispersity of the polymers were determined by Gel permeation chromatography (GPC). Polydispersity index (PDI) gave us the estimate of the heterogeneity (presence of molecules of different size and weight) in a sample.

Table 2: MW, size and PDI values of HPG, HPG+1S and HPG+3S determined by GPC.

	MW (x 10 ³) (g/mol)	Size (nm)	PDI
HPG 3K	2.717 (± 2.9%)	1.21 (±1.679%)	1.29 (± 3.029%)
HPG 3K with 1 GalNAc group (HPG+1S)	3.538 (± 1.7%)	1.25 (±6.197%)	1.29 (± 1.919%)
HPG 3K with 3 GalNAc groups (HPG+3S)	4.756 (± 1.8%)	1.46 (±1.85%)	1.38 (± 0.95%)

Table 1 shows the MW, size and PDI of all the three polymers synthesized. The MW of the polymer are an average and deviate from the empirical MW estimated.

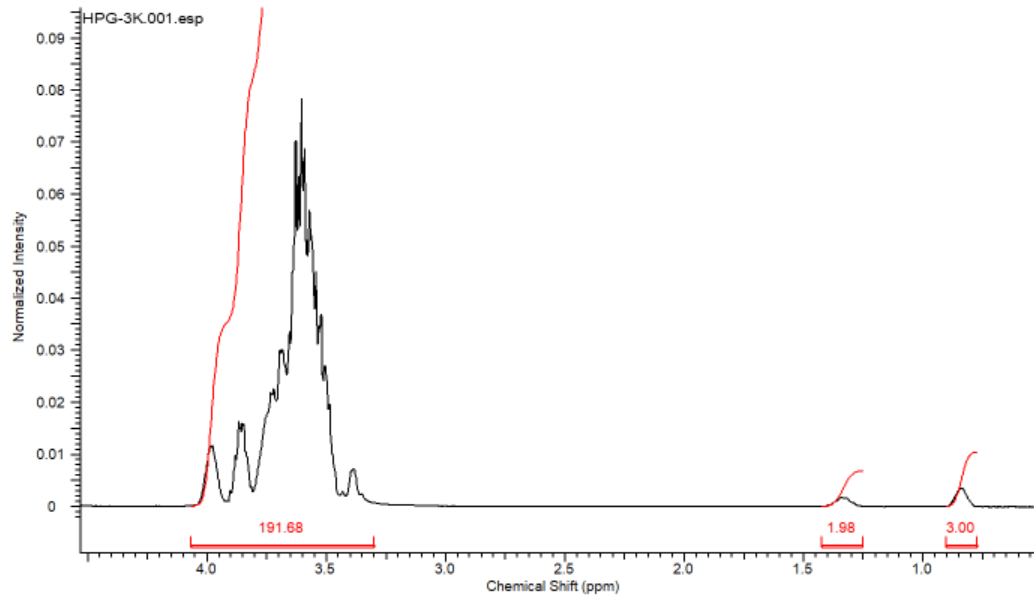


Figure 13: NMR of HPG 3K

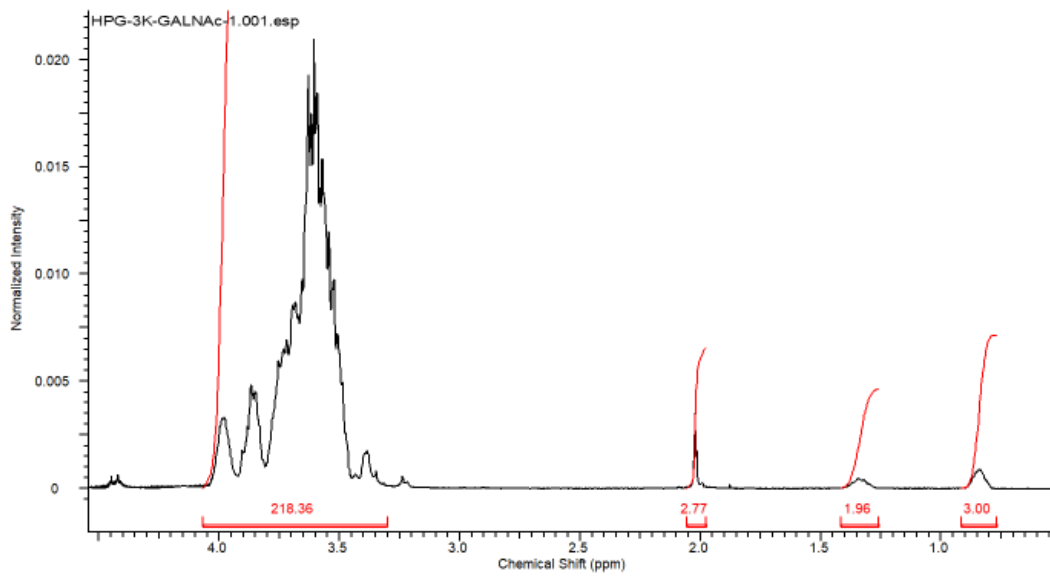


Figure 14: NMR of HPG 3K with one GalNAc group (HPG+1S)

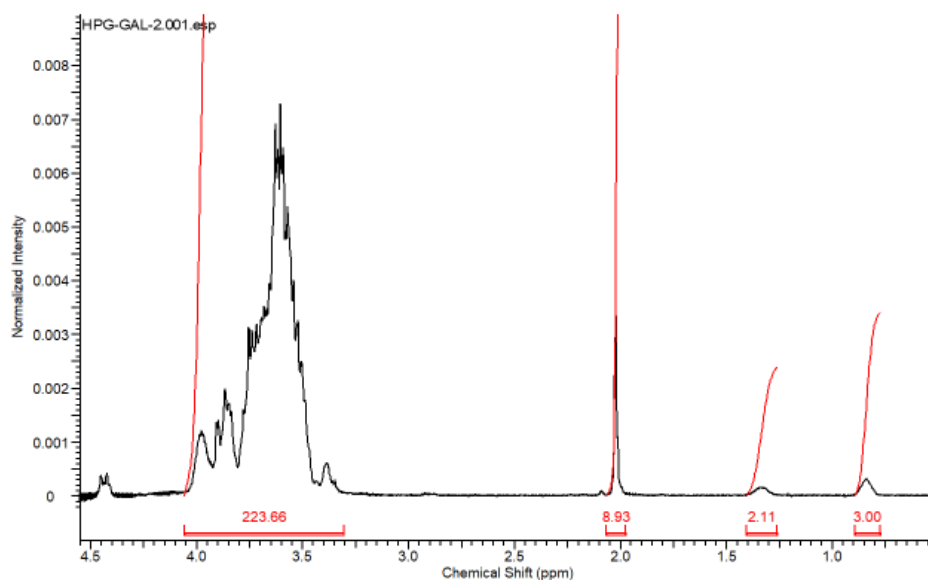


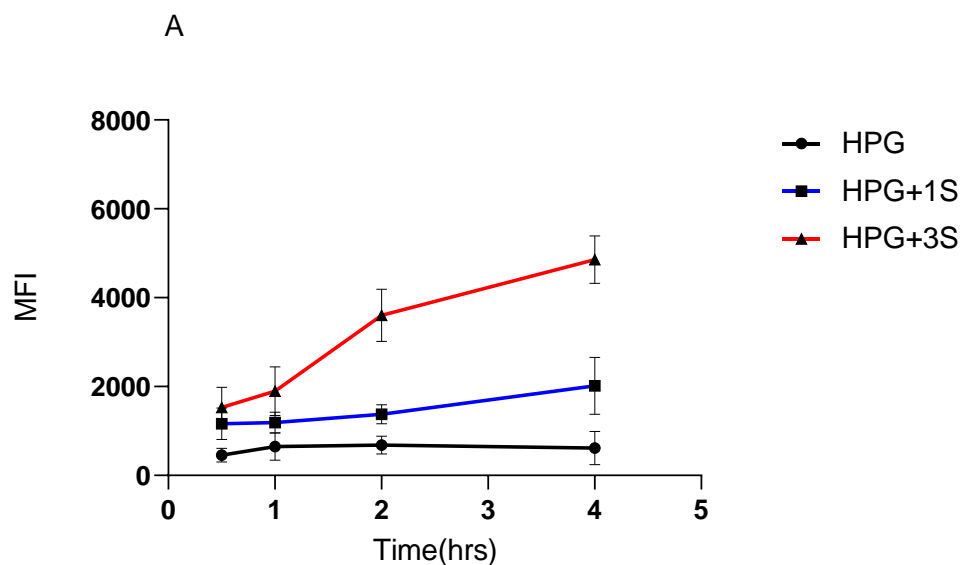
Figure 15: NMR of HPG 3K with three GalNAc groups (HPG+3S)

The peaks at 0.85, 1.3 and 3.25-4.1 ppm were characteristic proton peaks of the HPG. The peak at 0.85 ppm corresponds to the three protons present of the first CH₃ of the HPG polymer chain. The peak at 1.5 ppm showed the protons present in a CH₂ molecule. The peaks from 3.25 to 4.1 corresponded to protons of CHO molecules in the HPG polymer. There would be an overlap of protons from the GalNAc sugar group as well in these peaks. In Figures 14 and 15, another peak at 2.0 ppm was seen. This peak exclusively corresponded to the CH₃ group of the sugar. The difference in the chemical shift was due to the difference in the environment that the CH₃ groups are present. Thus, the presence of a peak at 2.0 ppm indicated the presence of GalNAc group. The integration values represent the number of protons available and hence to calculate the number of GalNAc groups presented per molecule, the integral values of peak at 2.0 ppm were divided by integral values of peak at 0.85 ppm.

4.2 In vitro examination of HPG and GalNAc conjugated HPG

4.2.1 Initial screening of polymer internalization in different hepatocyte cell lines

After characterization and dye tagging of the different HPG polymers and polymer conjugates, the efficiency of polymer conjugates uptake was tested in cultures of a panel of human hepatocytes (HepG2, HuH7.5.1 and THLE2). Since the polymer and polymer conjugates differed in the number of sugar moieties they carried, HPG referred to unmodified parent HPG (3k), HPG+1S referred to HPG 3K with an average of 1 GalNAc group per HPG molecule, and HPG+3S referred to HPG 3K having an average of 3 GalNAc groups per HPG molecule.



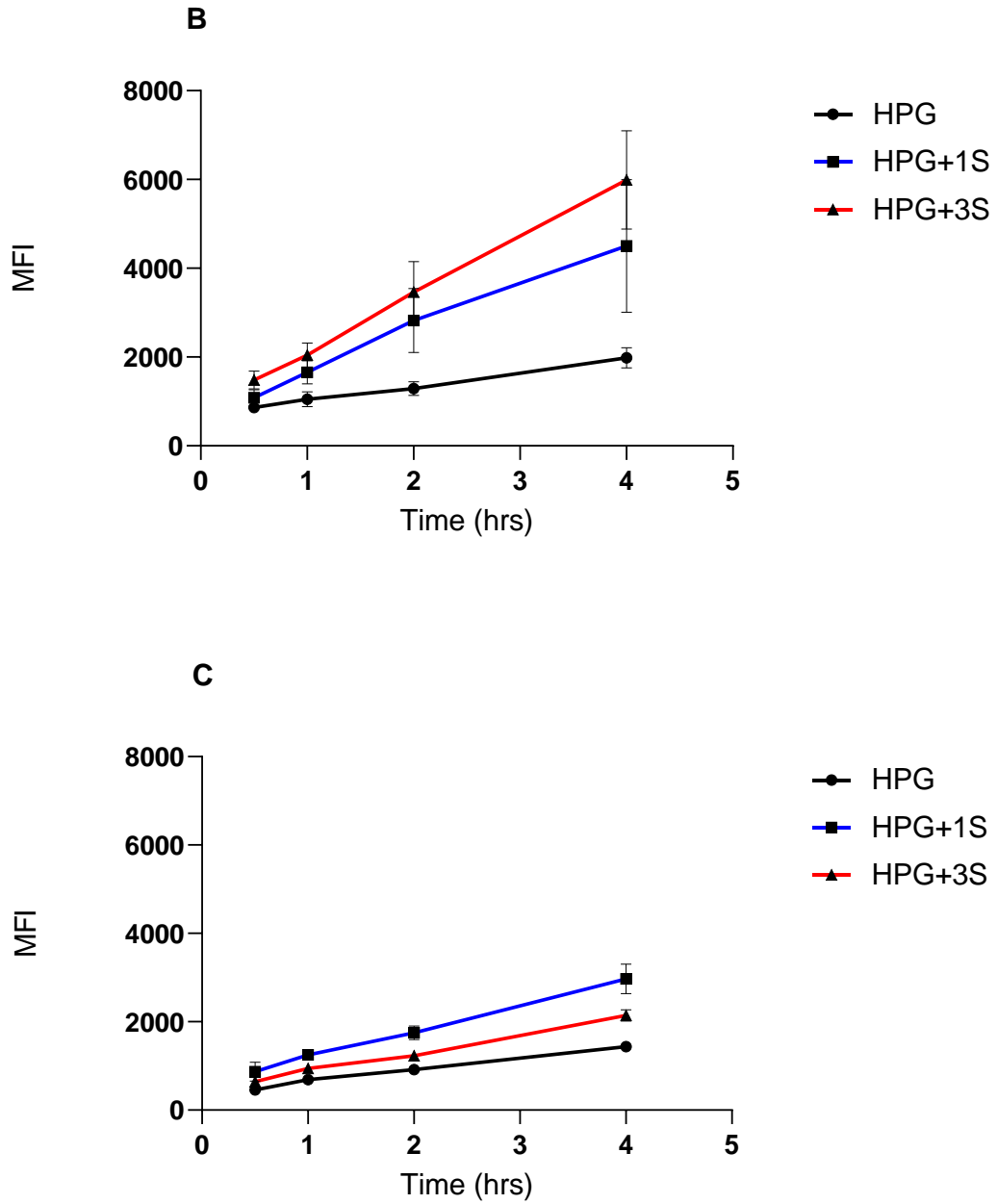


Figure 16: Time dependent internalization of Alexa 647 tagged HPG+3S, HPG+1S, and HPG in three hepatocyte cell lines using flow cytometry. A) In HepG2 cells. B) In HuH7.5.1 cells. C) In THLE2 cells.

From Figure 16, HepG2 cells showed significant uptake of HPG+3S than HPG+1S and HPG, indicated by both $p = 0.0049$ at 0.5 hour and $p = 0.0010$ at 1 hour (HPG+3S versus HPG), $p < 0.001$ at 2 hours (HPG and HPG+1S versus HPG+3S) and $p = 0.002$ at 4 hours (HPG versus HPG+1S). In HuH 7.5.1 cells (Figure 16B), a significant difference in the uptake of the polymers only after 2 hours could be seen, indicated by that $p = 0.0087$ (HPG versus HPG+1S) and $p = 0.002$ (HPG versus HPG+3S) at 2 hours, and $p < 0.0001$ at 4 hours in both the groups, additionally $p = 0.0111$ at 4 hours (HPG+1S versus HPG+3S), whereas in HepG2 cells the difference was visible from 30 minutes itself. In THLE 2 cells, HPG+1S performed better, which was indicated by $p = 0.0003$ at 1 hour (HPG+1S versus HPG). After 2 hours, all the polymers showed significant uptake, supported by $p < 0.0001$ (HPG versus HPG+1S), $p = 0.045$ (HPG versus HPG+3S) and $p = 0.0007$ (HPG+1S versus HPG+3S), and $p < 0.0001$ at 4 hours in all the groups.

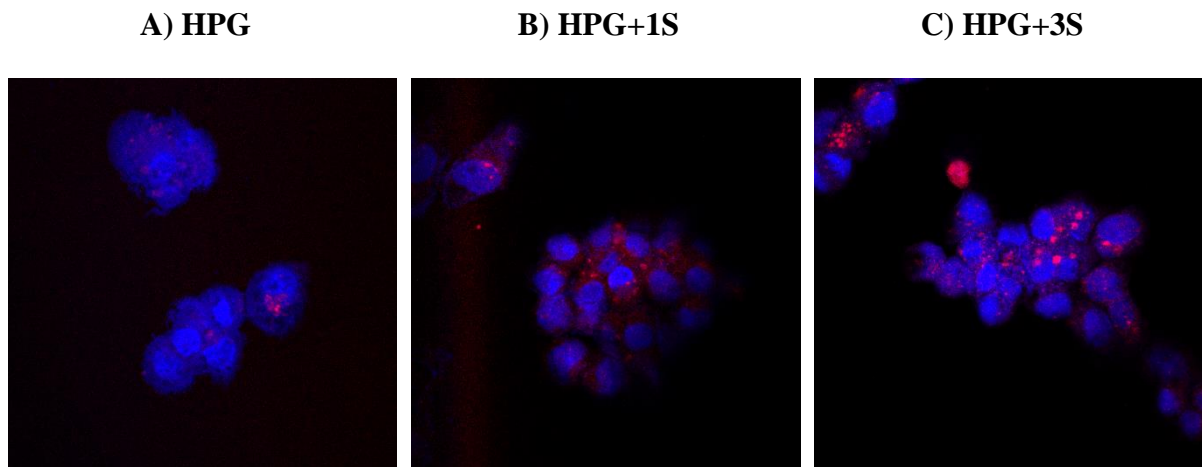


Figure 17: Polymer internalization in HepG2 cells fixed using 4%PFA in culture slides.

A) Red, HPG; blue, DAPI nuclei staining. B) Red, HPG+1S; blue, DAPI nuclei staining. C) Red, HPG+1S; blue, DAPI nuclei staining.

Confocal microscopy of fixed HepG2 cells which were priorly exposed to HPG, HPG+1S and HPG+3S (Figure 17) qualitatively showed that the amount of HPG+3S internalized was

comparatively more than HPG+1S and HPG; reaffirming data from previous studies that increased number of sugar moiety increases the uptake efficiency of polymer conjugates.

4.2.2 Receptor mediated internalization of HPG+3S.

The following results were from experiments designed to prove that internalization of GalNAc conjugated HPG in hepatocytes was ASGPR-dependent.

4.2.2.1 ASGPR expression in different human hepatocyte cell lines.

Panel of hepatocytes were stained for presence of ASGPR1 to know the amount of ASGPR expressed in each cell line. ASGPR1 antibody was sufficient to verify expression since ASGPR2 lacks export signal and cannot be expressed on the surface of a cell without ASGPR1(57).

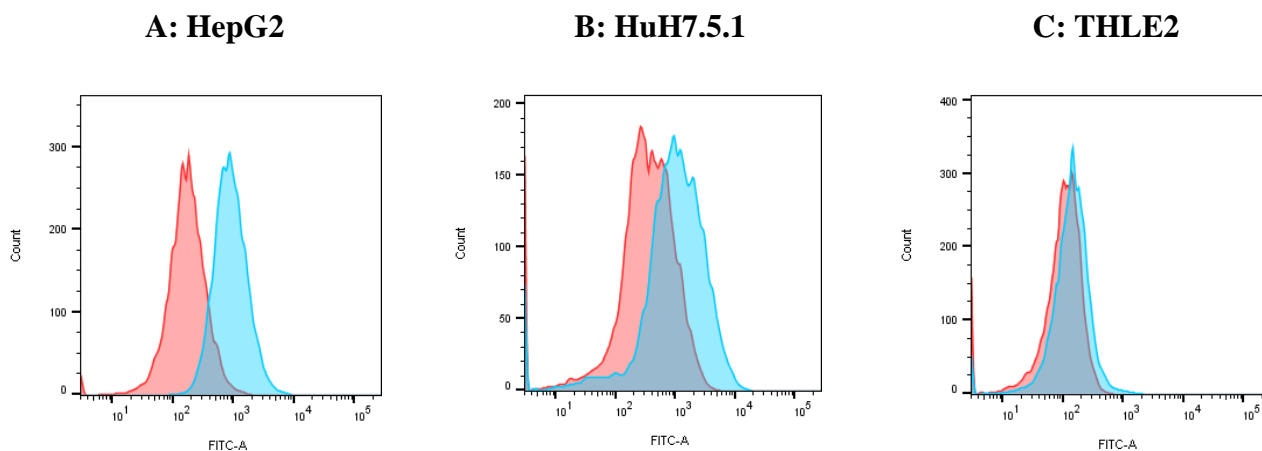


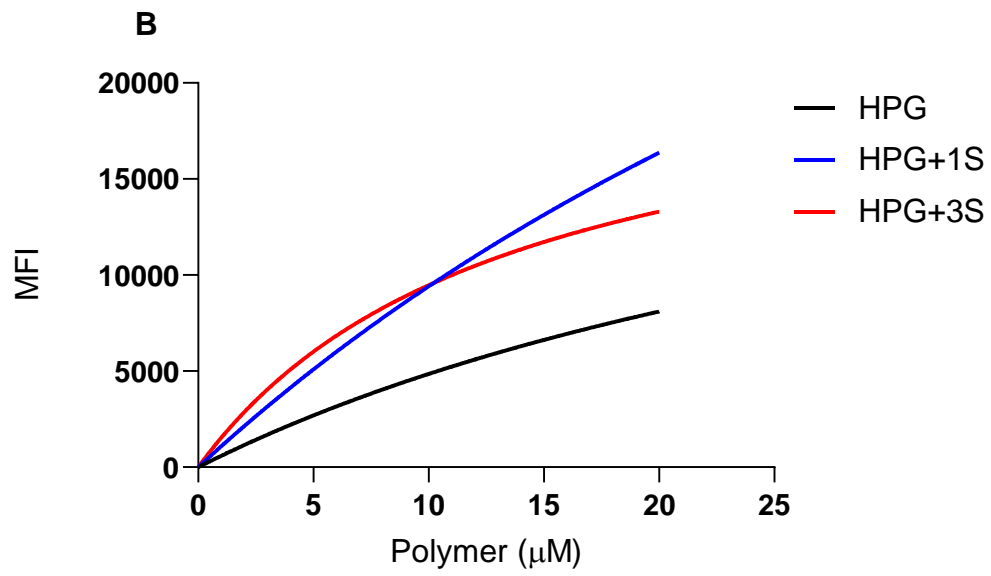
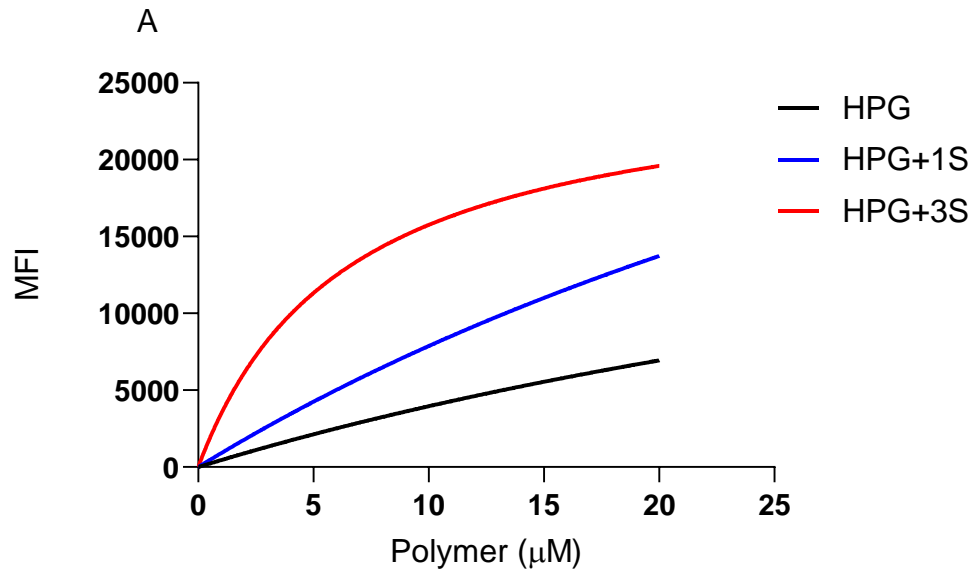
Figure 18: ASGPR1 receptor staining in different human hepatocyte cell lines using flow cytometry. Red: background staining, Blue: ASGPR1 staining. A) HepG2 cells: high expression. B) HuH7.5.1 cells: moderate expression. C) THLE2 cells: low expression.

The histograms of cells that were stained for the receptor were merged with the histograms of the cells that background stained. The area under the curve in red corresponded to the cells that were background (isotype antibody) stained, and blue referred to the cells that

were stained (positive). Amongst the chosen hepatocyte panel high expression of ASGPR was seen in HepG2 cells, followed by moderate expression in HuH.7.5.1 cells. Interestingly, in THLE2 cells, low expression of ASGPR1 was observed. When the difference of MFIs between the stained group versus control group were compared a similar pattern was observed, with the difference in HepG2 cells being the greatest (531.5), followed by HuH7.5.1 cells (275) and the difference in THLE2 cells being the smallest (50).

4.2.2.2 Determination of affinity of polymer conjugates and dose dependent internalization.

After obtaining ASGPR expression in different hepatocyte cell lines, we examined the uptake of unmodified HPG and its polymer conjugates in these cell lines. The cells were incubated with fluorescent labeled polymer conjugates for a period of two hours and analyzed with the help of FACS. MFI values were plotted against concentration to draw a non-regression Michaelis-Menten kinetics curve. Usually, the Michaelis-Menten curve is drawn using concentration on X axis and the rate of internalization on Y axis. Since it was difficult to figure out the rate of internalization, K_m values were obtained using MFI values through non-linear regression plots using Graphpad8 software.



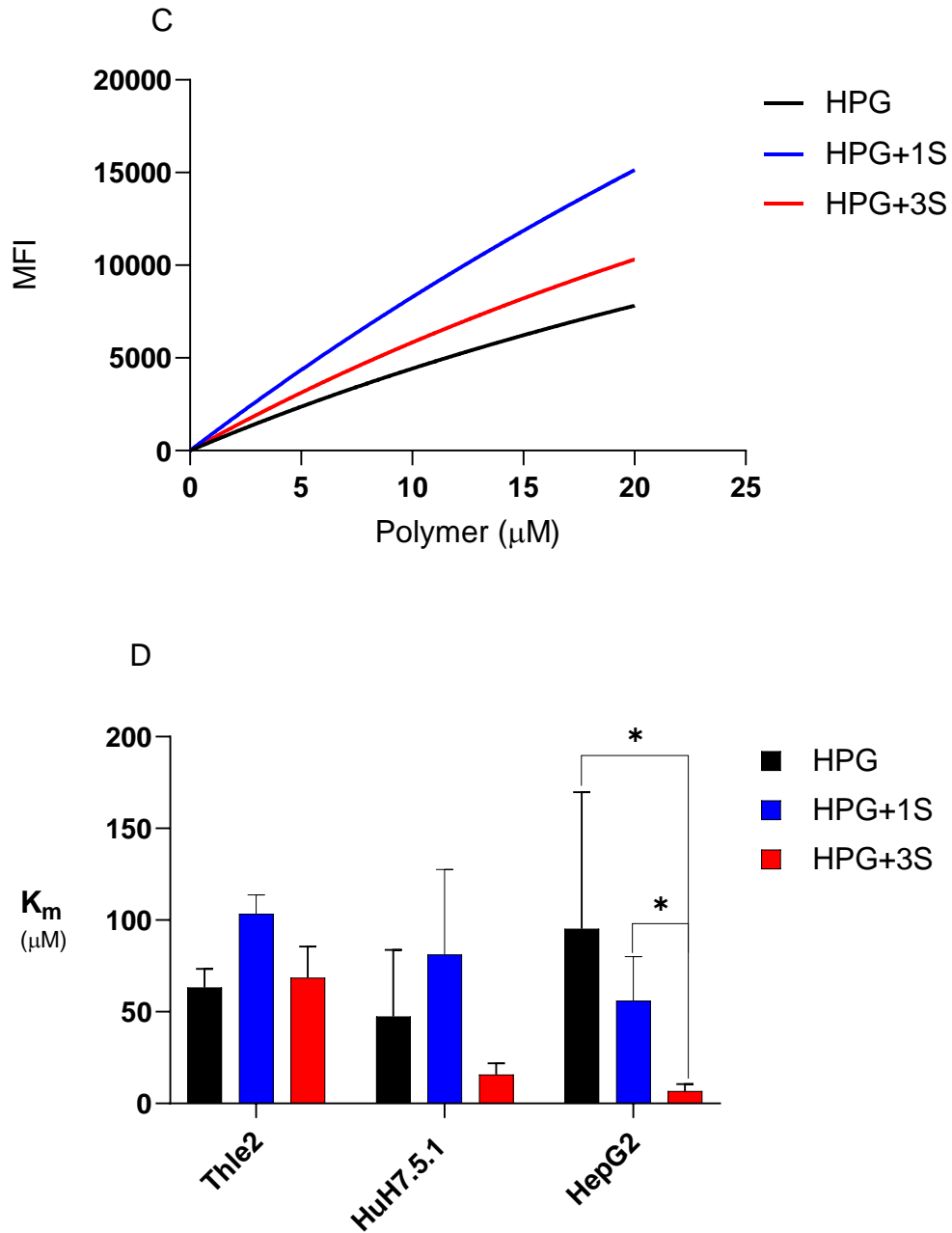


Figure 19: Determination of affinity of HPG polymer and polymer conjugates using flow cytometry. A) Dose dependent response in HepG2 cells. B) Dose dependent response in HuH7.5.1 cells. C) Dose dependent response in THLE2 cells D) Comparison of K_m values across the hepatocyte cell lines panel.

Multiple comparison using two-way ANOVA that in HepG2 cells, HPG+3S performed better than HPG+1S and HPG ($p = 0.0196$ and $p < 0.0001$, respectively), HPG+1S showed better internalization than HPG ($p = 0.035$) at their highest concentrations. At 2 μM , HPG+3S showed significant uptake than HPG ($p = 0.0467$). In HuH7.5.1 cells also HPG+3S showed better uptake with higher concentrations than HPG with $p < 0.0001$ and HPG+1S with $p = 0.0058$. In THLE2 cells as well there was significant difference in the MFI values between the unmodified HPG polymer and polymer conjugates at higher concentrations. Table 3 shows the K_m values of the polymers in all three hepatocyte cell lines.

Table 3: Mean K_m values of the polymer candidates in hepatocyte cell lines.

	HPG (μM)	HPG+1S (μM)	HPG+3S (μM)
THLE2	65.86	95.83	66.14
HuH7.5.1	40.50	56.66	13.57
HepG2	61.05	58.24	6.44

From table 3, it was seen that K_m values were lower for HPG+3S in the cells that express ASGPR at least moderately. The lowest K_m value was 6.44 micromoles in HepG2 cells. This indicated that HepG2 cells and HPG+3S would make an ideal model for further studies.

4.2.2.3 Uptake in Kidney Cells that Ectopically Express ASGPR

To confirm that internalization of HPG+3S was through the ASGPR and not through some other sugar binding receptor, HEK293 cells which are human embryonic kidney cells that normally do not express the ASGPR were used. Three groups of cells were used:

1. Cells that did not express both ASGPR1 and ASGPR2 genes (ASGPR^{-/-})
2. Cells that expressed only ASGPR1 but not ASGPR2 (ASGPR^{+/-})
3. Cells that expressed both ASGPR1 and ASGPR2 (ASGPR^{+/+})

All the three cell lines were stained to check expression of ASGPR1.

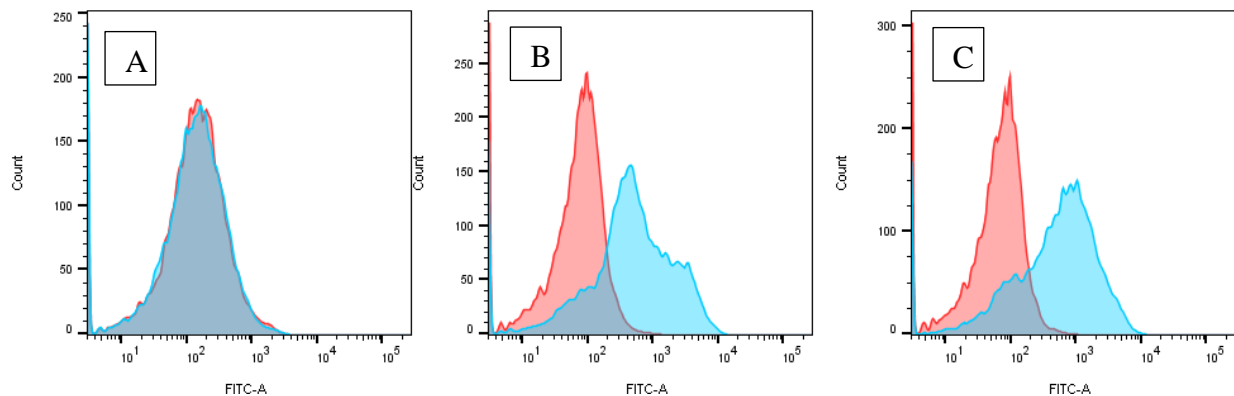


Figure 20: ASGPR1 receptor staining in HEK293 cells using flow cytometry. Red: background staining, blue: ASGPR1 staining. A) ASGPR^{-/-} B) ASGPR^{+/-} and C) ASGPR^{+/+}.

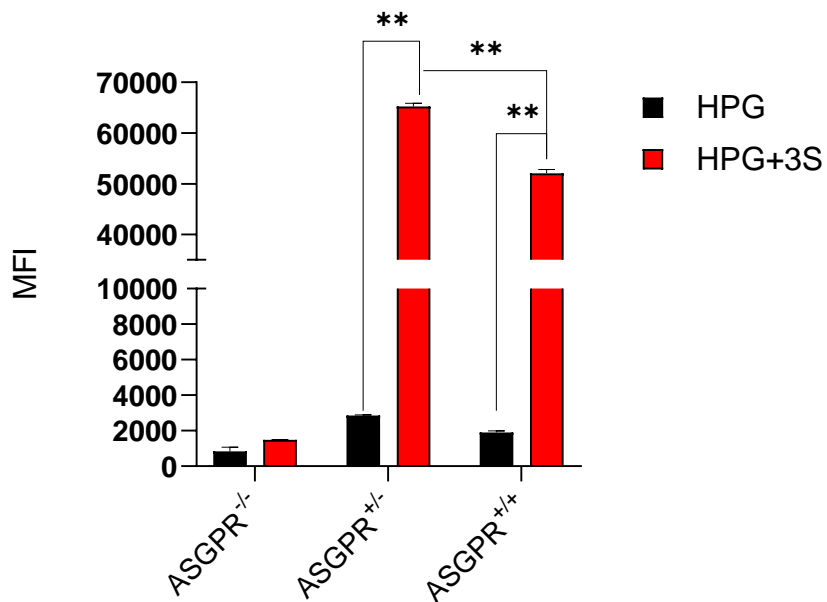


Figure 21: Uptake analysis of HPG and HPG+3S in HEK293 cells using flow cytometry.

ASGPR^{-/-}: HEK 293 cells, ASGPR^{+/-}: HEK293 cells expressing ASGPR1 gene,

ASGPR^{+/+}: HEK293 cells expressing ASGPR1 and ASGPR2 gene.

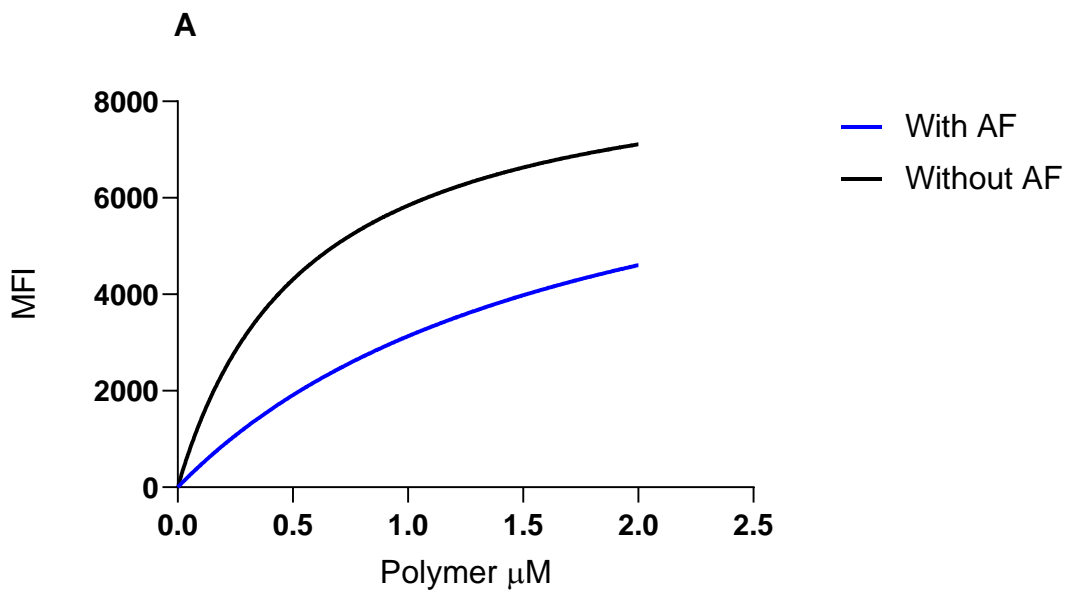
Comparing MFI values of HPG and HPG+3S, a significant increase was observed in HPG+3S uptake in both ASGPR^{+/-} and ASGPR^{+/+} ($p < 0.001$ during multiple comparison tests of two-way ANOVA) over HPG. For HPG+3S, ASGPR^{+/-} had higher MFI values than ASGPR^{+/+} (with $p < 0.001$, unpaired T test).

4.2.2.4 Competitive Inhibition with Natural Ligands

Asialofetuin:

To further confirm ASGPR mediated uptake of HPG+3S, a competitive inhibitory experiment was done with the flow cytometry. HepG2 cells were exposed to HPG+3S with and without asialofetuin (natural ligand for ASGPR) and K_m values were calculated. Our results show that competitive inhibition of HPG+3S with asialofetuin resulted in the increase in K_m

values of HPG+3S. In the presence of asialofetuin, the K_m values of HPG+3S was 1.77 ± 0.54 μM whereas in the absence of asialofetuin the K_m value was 0.555 ± 0.27 μM . The results were significant with $p = 0.0024$. The percentage of inhibition was close to 50% with a 1:4 ratio of HPG+3S to asialofetuin. Inhibition percentage was found to increase with increasing ratios initially and then eventually decreased with the mean value of percentage inhibition being 61% amongst the concentrations used with one sample test $p < 0.001$.



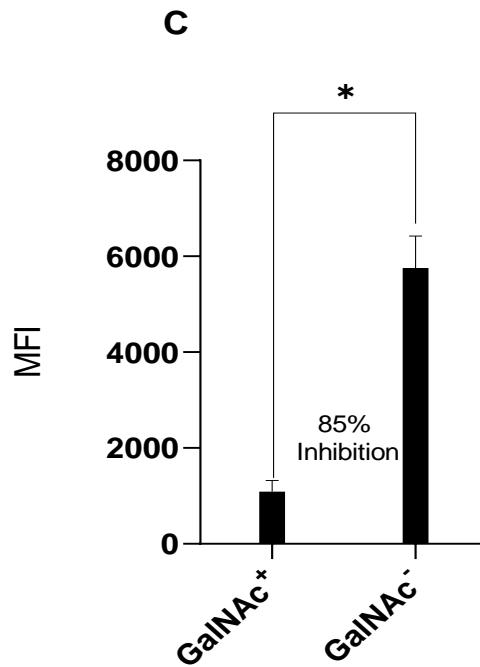
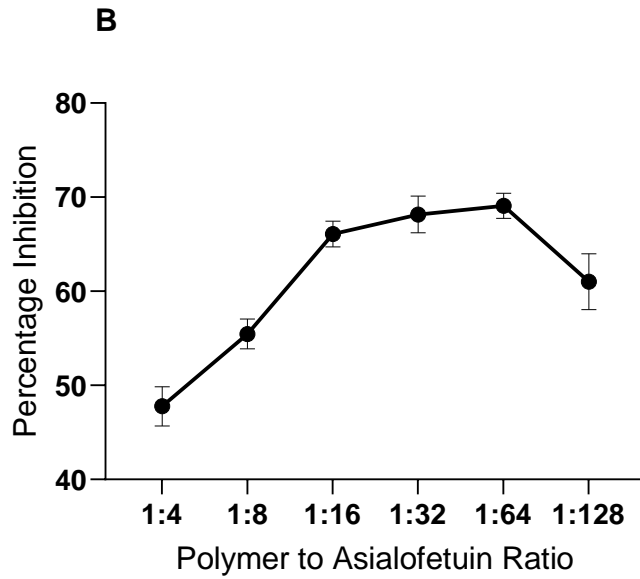


Figure 22: A) Competitive Inhibition of HPG+3S using flow cytometry in the presence and absence of asialofetuin. B) Percentage inhibition of uptake of HPG+3S by asialofetuin. C) Competitive inhibition of HPG+3S by GalNAc using flow cytometry.

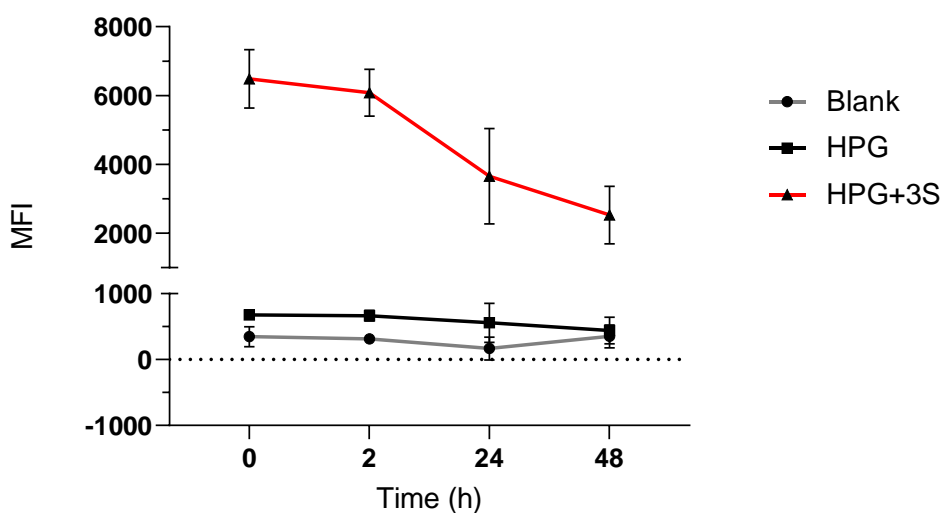
GalNAc:

Competitive inhibition with GalNAc was also performed to reaffirm the above results. HepG2 cells were exposed to HPG+3S in the presence and absence of naturally occurring GalNAc. There was around 85% of inhibition of HPG+3S by GalNAc with a polymer to GalNAc ratio of 1:10,000, confirming that HPG+3S uptake by hepatocytes was indeed through the ASGPR with paired t-test $p = 0.0067$.

4.2.3 Efflux of HPG+3S from Hepatocytes

It was necessary to know if the internalized polymer conjugate is eventually effluxed out of the hepatocytes since we expect HPG+3S to enter the biliary route and be eliminated via feces. HepG2 cells were initially treated with HPG+3S and HPG for 2 hours and later washed and switched to fresh media. A decrease in the MFI values was observed after the cells were switched to fresh media (Figure 23). There was not much difference between blank (no treatment) and HPG group.

Figure 23: Efflux of HPG polymers in HepG2 cells after 2 hours of treatment.



A significance with $p = 0.005$ was obtained when values were compared by two tailed t-test suggesting HPG+3S internalization as well as efflux.

4.2.4 Internalization by Monocytes

THP-1 cells were stained for the antibody and MFI value was 246 after normalizing values with the background. Cells stained positive which meant there was a low level of ASGPR expression in THP-1. Figure 24 shows the staining of THP-1 cells with side-by-side comparison with HepG2 cells.

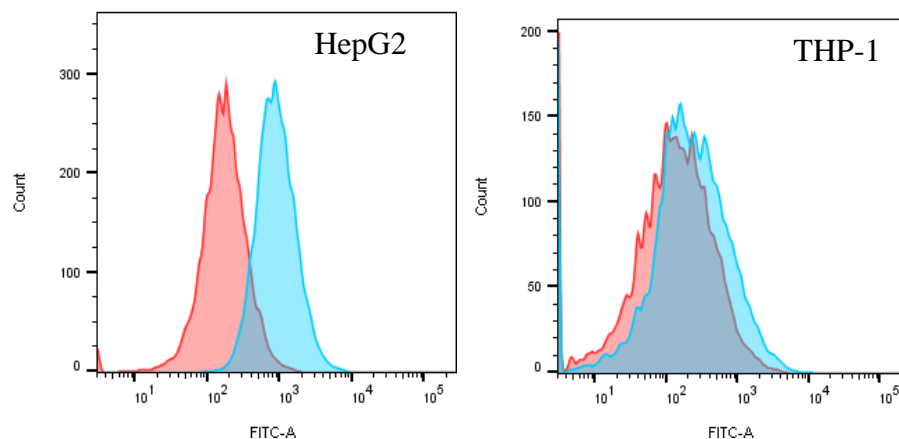


Figure 24: Comparison of receptor expression in hepatocytes (HepG2) vs monocytes (THP-1) Red: background staining, blue: ASGPR1 staining. HepG2: High expression, THP-1: low expression.

THP-1 cells were then treated with HPG polymers for up to 4 hours and internalization was analyzed. It was seen that there was a significant difference in uptake between HPG+3S and HPG ($p = 0.008$, Two tailed t-test). When the results of THP-1 were compared to that of

HepG2, it was seen that HPG+3S uptake in HepG2 was significantly higher when compared to THP-1 ($p = 0.0037$ at 2 hours, $p < 0.0001$ at 4 hours).

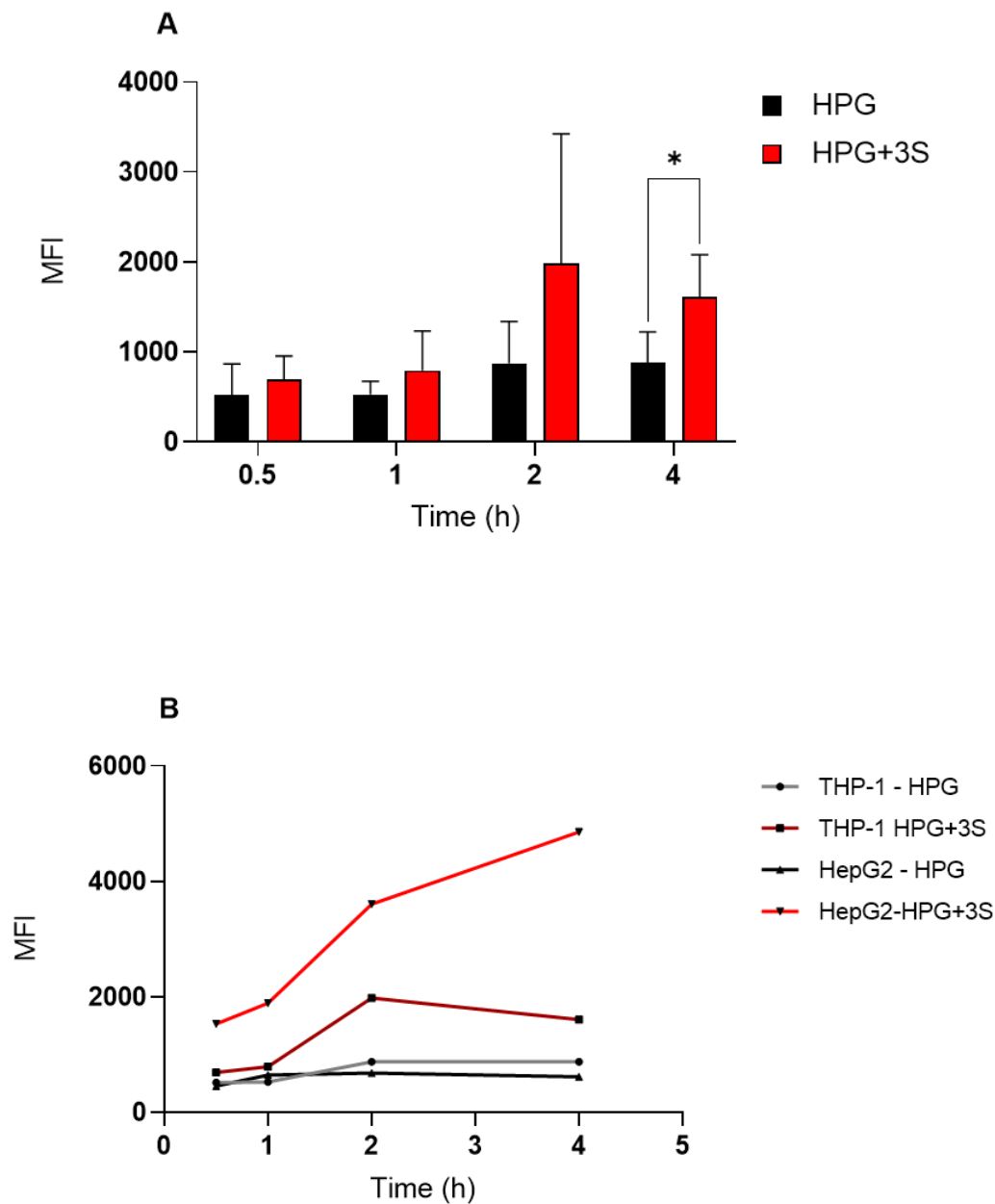


Figure 25: A) Time dependent uptake of HPG polymers in THP-1 cells. B) Comparison of uptake of HPG polymers in THP-1 and HepG2 cells.

4.3 Biodistribution of HPG and HPG+3S in mice

To understand what happens to HPG+3S and where it goes in vivo, we intravenously injected mice with radiolabeled HPG+3S and HPG, monitored the mice up to 48 hours, collected various organs, and their homogenate was analyzed for radioactivity to compare biodistribution of the polymer with and without GalNAc modification. The data here is organized based on different organ systems in the animals with more emphasis on the digestive system and urinary system since we expected to see significant difference in these two systems more than the others.

4.3.1 Digestive System

Under the digestive system, stomach, small and large intestines, gall bladder and the liver were collected. Most of the organs of the digestive system were the organs encompassed by the peritoneum and thus it was necessary to see the percent of injected dose retained in this system. Our results were on par with our hypothesis and confirmed that HPG+3S conjugation facilitated uptake by the liver. Statistical analysis also proved to be significant (HPG+3S vs HPG, $p = 0.0025$, two tailed t-test). The percentage of HPG+3S retained in the liver when compared to all the other organs across all the other systems was higher and greater than the percent of HPG retained in the liver. HPG+3S passes through the biliary route because Figure 26 B shows an increase in the percent of injected dose of HPG+3S excreted, especially between 8-24 hours. In 48 hours, approximately 17% of the injected HPG+3S was excreted via the feces but not even 2% of the unmodified polymer (HPG) was excreted via feces ($p = 0.0027$).

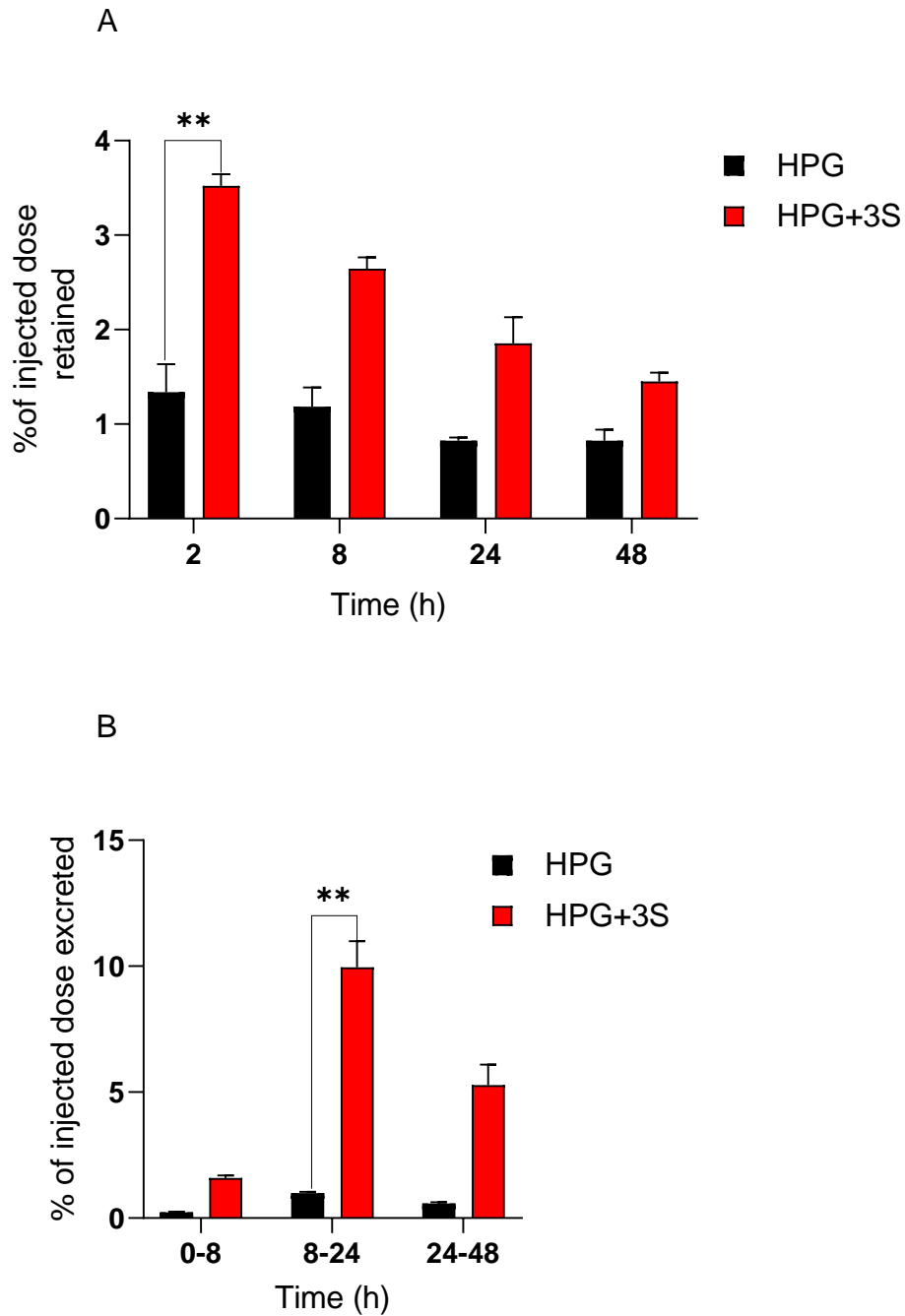


Figure 26: Distribution of HPG compared to HPG+3S for 48 hours. A) Percent of injected dose retained in the Liver. B) Percent of injected dose excreted out through feces.

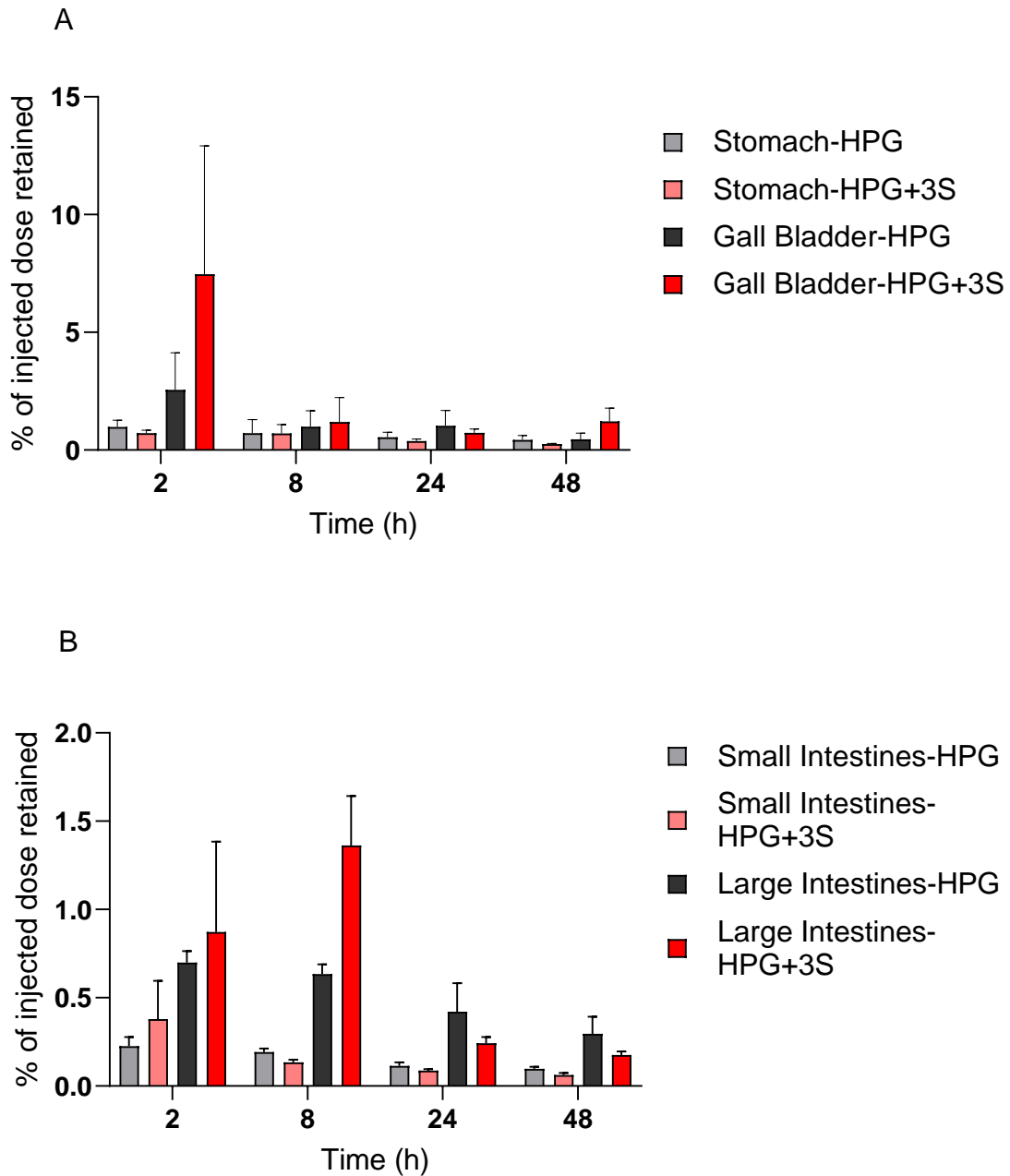


Figure 27: Distribution of HPG compared to HPG+3S in organs of the digestive system. A) Percent of injected dose retained in stomach and Gall bladder. B) Percent of injected dose retained in the small and large intestine.

Roughly around the same time, a spike in the intestine (Figure 27 B) was seen as well, but this was not statistically significant ($p > 0.5$). At 2 hours, there was comparatively some HPG+3S retention in the gall bladder. Unfortunately, these data were not statistically significant ($p = 0.25$). Similarly, in the stomach, there was no significant difference in the amount of polymer retained between the two groups ($p = 0.06$).

4.3.2 Urinary System

The kidneys are responsible for urine production and the clearance of molecules from the circulatory system. Up to 24 hours, it was seen that ~1 % of the injected dose was retained in the kidneys with no significant difference between HPG and HPG+3S ($p = 0.25$). On the other hand, we saw the percent of injected dose excreted via the urine, more than 80% of the injected HPG was excreted within a span of 24 hours and about 65% of injected HPG+3S was excreted in the HPG+3S group. There are no error bars in Figure 28 B because of the difference in collection of samples between both the groups. In our experiments, an increased liver uptake of HPG+3S despite the animals having a normal functioning renal system that flushed out the polymer was noticed. In the HPG+3S group, about 17% of the polymer was excreted via the feces and the rest (~65%) was out through the urine.

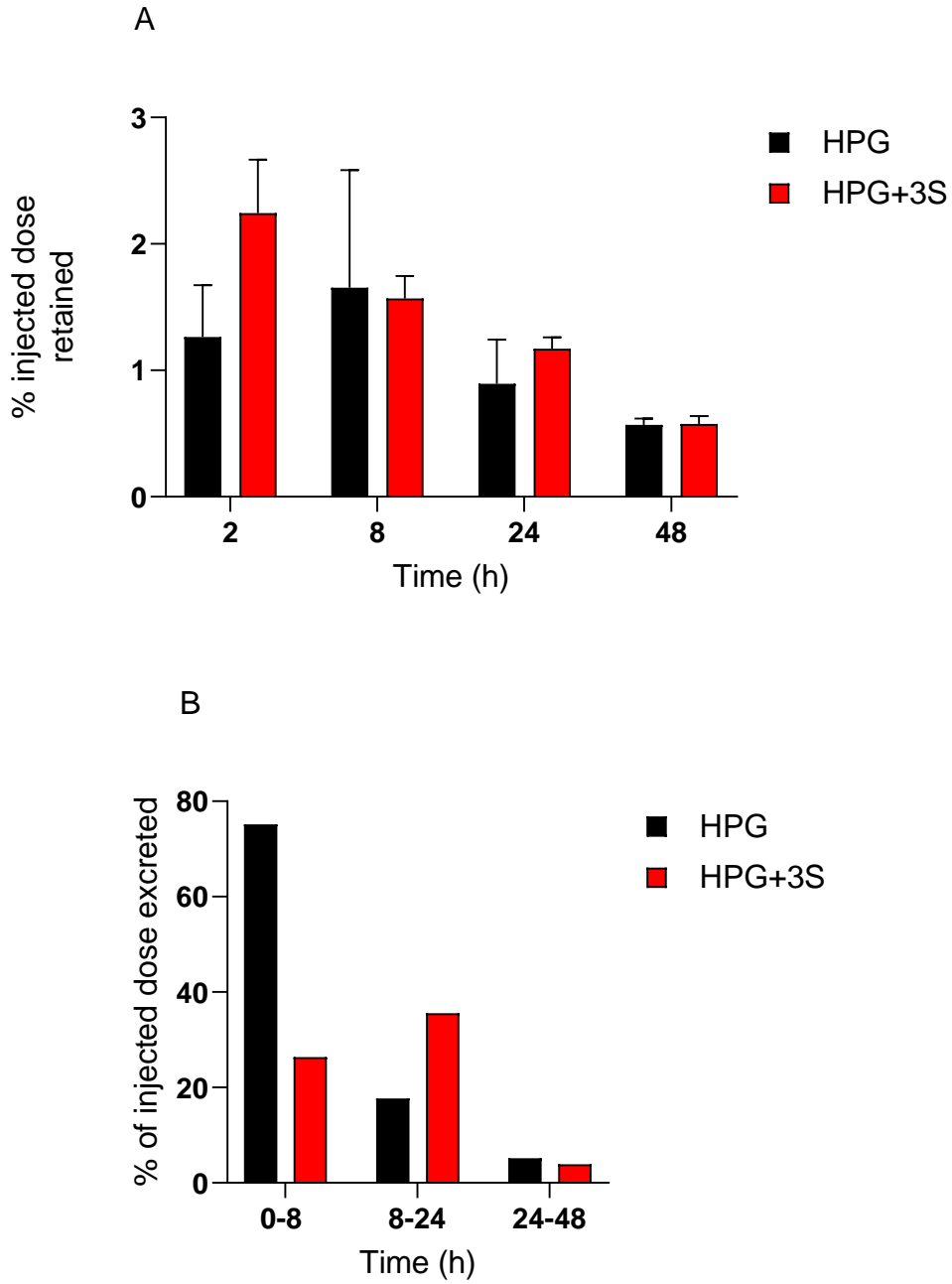
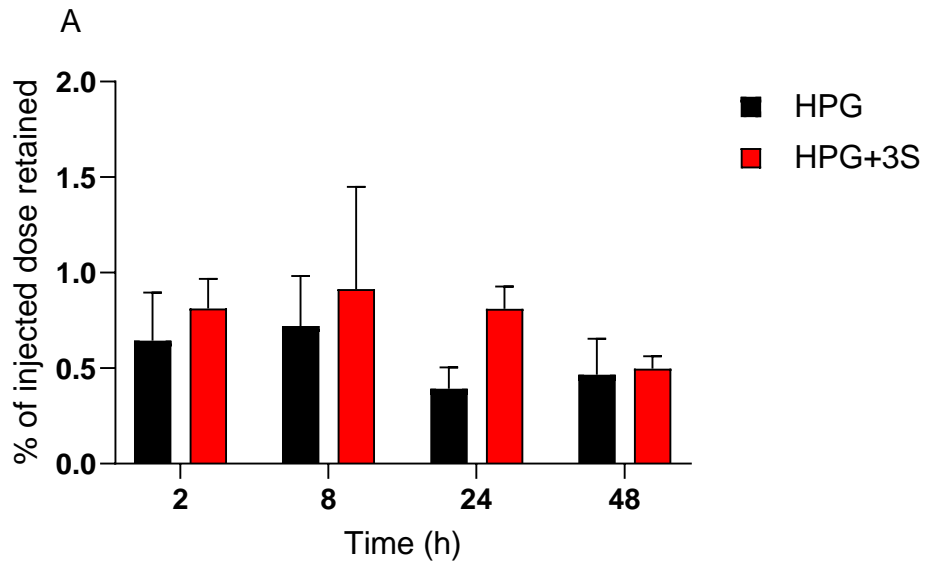


Figure 28: Distribution of HPG and HPG+3S in the urinary system. A) Percent of injected dose retained in the Kidney. B) Percent of injected dose excreted via Urine.

4.3.3 Circulatory System

For the circulatory system, distribution in the heart, whole blood as well as plasma and spleen were analyzed. Overall, there was no significant difference in the percentage of HPG and HPG+3S accumulated in the heart and spleen but at 8 hours and 24 hours there was a significant difference with $p = 0.0023$ and $p = 0.03$, respectively. In whole blood and plasma there was a significant difference in the ratios between HPG and HPG+3S solutions ($p = 0.0068$, two tailed T test). Although there was significance in the presence of HPG+3S in the blood, the percentage of injected HPG+3S retained was still very low and around 2% in the plasma at 2 hours but overall, around 1% only remaining after two hours.



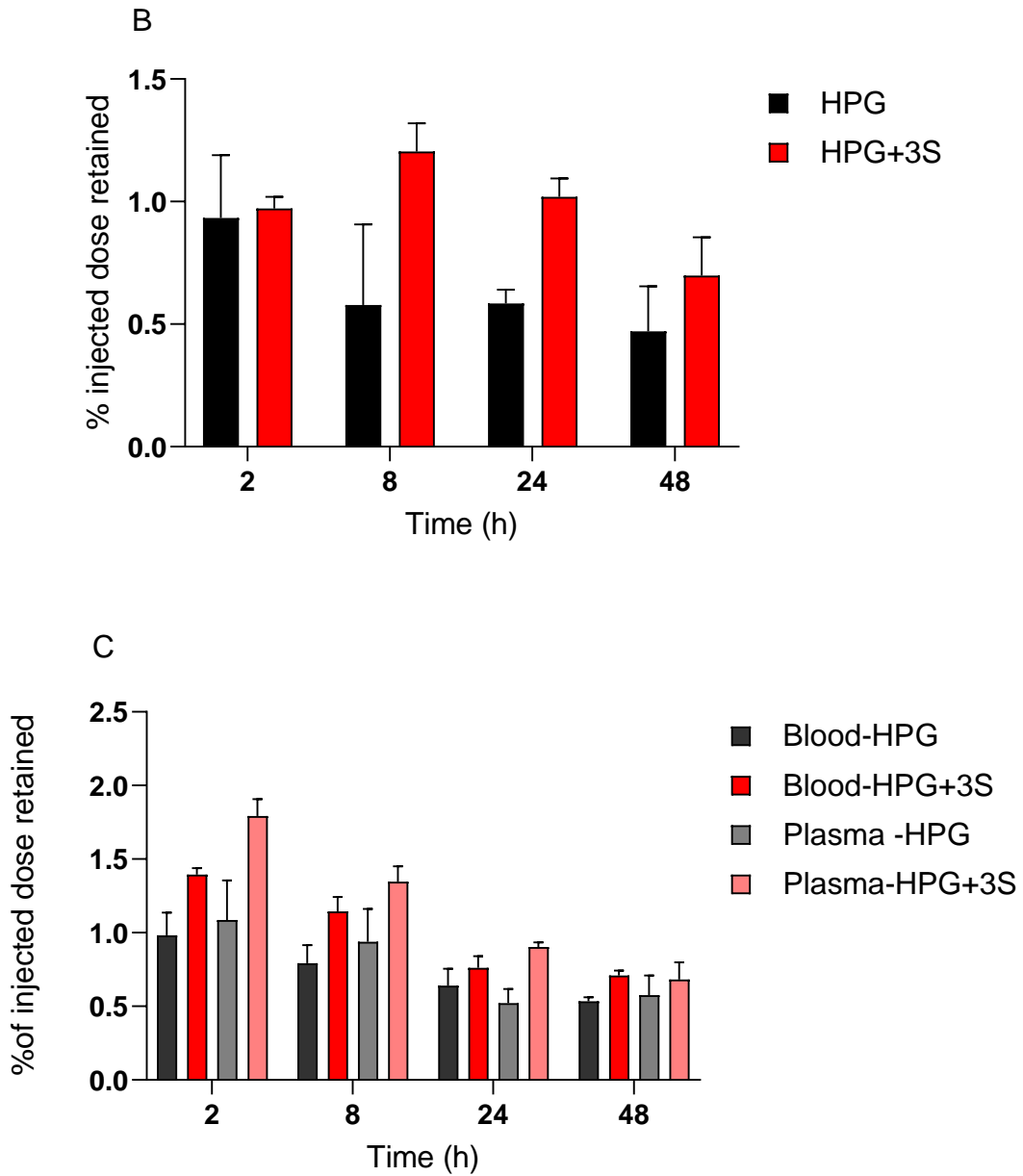


Figure 29: Distribution of HPG and HPG+3S in the circulatory system. A) Percentage of injected dose retained in the heart. B) Percentage of injected dose retained in the spleen. C) Percentage of injected dose retained in the whole blood and plasma.

4.3.4 Respiratory System

In Figure 30, at 2 hours, approximately 1.5% of injected HPG+3S is found in the lungs compared to 0.5% of HPG, but by 48 hours HPG+3S percentage drops to 0.5%. This showed that HPG+3S was being either phagocytosed or redirected to the liver. On the other hand, the percent of HPG retained remained quite constant at all time points (a little above 0.5%) although not at a greater level. Two tailed t-test values for both the polymers were not significant ($p = 0.5$).

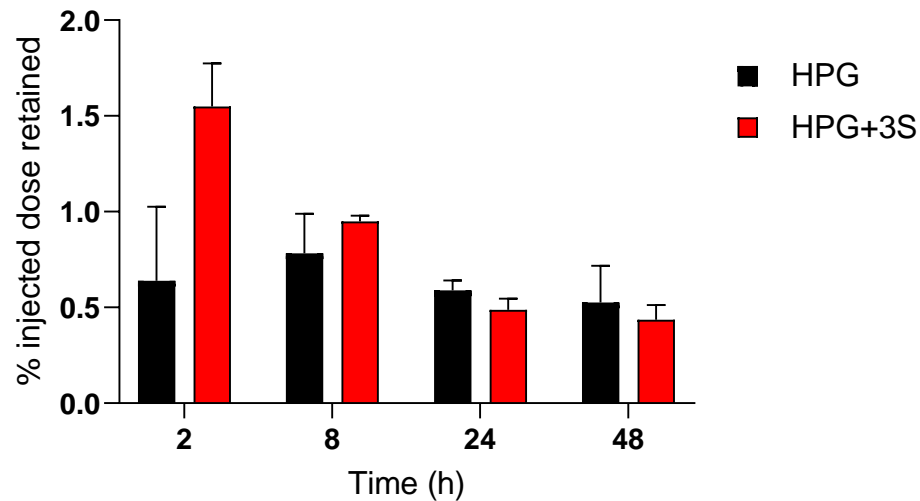


Figure 30: Percent of injected dose retained in the lungs.

Chapter 5: Discussion

5.1 Synthesis and Characterization of HPG polymers

The results of characterization of HPG-GalNAc polymers indicate that the experimental setup can be used for conjugation up to three sugar moieties per HPG molecule. Increasing the sugar to polymer ratio for conjugation of more sugar groups per HPG molecule resulted in 2-3 GalNAc groups repeatedly. This might be due to steric factors that GalNAc around a relatively small HPG core (HPG 3K) can be challenging to accommodate. The higher molecular weight HPG were able to be conjugated with greater than 5 GalNAc groups using click chemistry(71). However, click chemistry method was not tried for conjugation in our synthesis process. The molecular weights of the polymer deviate from the empirical molecular weights estimated. It is to be noted that the molecular weight of HPG polymers and number of GalNAc groups per HPG molecule is an average. Thus, polymer solutions are interspersed with molecules varying in molecular weight and size and GalNAc groups present. This must be kept in mind while interpreting the in vitro data. Dialyzing the final product for long hours decreased the polydispersity of the polymer solution but also led to increase in molecular weight. This is because the membranes used for dialysis have pores that cut off an average molecular weight/size and might contain bigger pores that will lead to some polymer loss. Hence dialyzing times had to be controlled. NMR spectra obtained were consistent to that previous reported data for HPG and presence of GalNAc was detectable in HPG+S and HPG+3S.

Fluorescent labeling reactions that were set up to generate a lower dye to polymer ratio which suggests that there is a chance that every HPG molecule might not have a dye conjugated to it. This could interfere in the in vitro results as more polymer molecules might be internalized than the amount quantified. Despite this, in vitro results were consistent for replicas of the

experiment performed. Hence for better accuracy, radiolabeling was preferred for in vivo experiments.

5.2 In vitro analysis of HPG polymers

Initial screening of the polymer in various hepatocyte cell lines (figure 16) is in accordance to our hypothesis that GalNAc conjugated HPG has greater uptake potential by hepatocytes than unmodified HPG. The difference in the uptake potential of HPG+S and HPG+3S in the three hepatocyte lines (HepG2, Huh7.5.1 and THLE2) can be attributed to various factors such as:

1. the number of GalNAc groups present.
2. the spatial alignment of the sugar groups
3. the steric hindrance of the molecules while binding with the receptor.
4. The amount and type of receptor expressed on the surface of cells.

Staining all these three cell types with ASGPR1 gave us a picture of how much difference in the expression of ASGPR amongst the chosen hepatocyte panel. Only ASGPR1 antibody was used because it has been proven previously that ASGPR2 lacks an export signal and it relies on ASGPR1 to be presented in the plasma membrane(57). THLE2 cells having originated from primary cells were expected to have the greater expression of the receptor(72), but we observed that the expression was much lower(Figure 18 C), which may be due to a high passage number of the cells (passage 38) when we received them from ATCC. The gene expression changes (up-regulated or down-regulated) can be expected following many passages in cultures. Also, THLE2 cells contain viral vectors and insertion of vector can also affect their gene expression.

From the dose response curves (Figure 19), we could see that HPG and HPG+S tend to have a more linear graph when compared to HPG+3S. This difference is stark in HepG2 cells

and can also be seen in HuH7.5.1 cells. ASGPR exists as a trimer on the cell surface and the presence of three GalNAc groups in HPG+3S might set out a perfect tri-antennary ligand for the receptor. Non-linear Michaelis-Menten kinetics analysis suggest HPG+3S follows receptor mediated uptake since K_m values are the least for HPG+3S especially in HepG2 cells. The lowest K_m value of HPG+3S is in HepG2 and the fact that HepG2 have a good expression of ASGPR were the reason why HepG2 cells were chosen as the best fit for 2D model for competitive inhibition experiments performed for this thesis. Although results of our uptake experiments suggest internalization of HPG+3S based on ASGPR expression similar to the results obtained by Zhou et al(73), there are a few caveats that we need to be aware of. We know that dye tagging of the polymer candidates was successful, but the reaction yield and efficiency is not 100%. This means that there is a good probability for untagged polymer molecules to be taken up by the hepatocytes but wouldn't contribute to fluorescence values. Once a molecule is tagged with a dye, it should be treated as a completely different molecule from the parent molecule as Alexa 647 itself has a molecular weight around 1 kDa. The best way to overcome this drawback is by radiolabeling polymer candidates. Due to safety concerns, the tedious processes involved with handling radiolabeled polymer and lack of facilities to use radiolabeled polymer for the in vitro studies, we chose to use fluorescent labeled polymer for the in vitro experiments and used radiolabeled polymer for the in vivo studies for better accuracy. MFI values were used as a parameter to determine internalization of polymer molecules, but Michaelis-Menten equation uses rate of internalization to calculate K_m values. This is not something new, and previous studies (57,69) have resorted to the same method as well. It should be kept in mind that K_m values calculated for the polymer candidates are arbitrary values indeed.

Contrastingly, in THLE2 cells, we saw that HPG+S shows better uptake than HPG+3S but the dose response showed a linear relation between concentration and uptake which does not suggest receptor mediated uptake. Even though, there are other non-specific modes of entry into the cell; for example: pinocytosis and diffusion through the plasma membrane are a couple of ways the polymer can enter the cell(74), it is unlikely that HPG would be able to diffuse through the plasma membrane considering its size. The other likely option that explains the uptake of HPG and HPG+1S is fluid-phase endocytosis that involves pinching off the sinusoidal surface of the cell(75,76). Also, HPG+S is smaller than HPG+3S but larger than HPG. Naturally, the next question that arose was why we did not see more of HPG uptake than HPG+S. This could be explained by the presence of GalNAc group in HPG+S, which might help in identifying HPG+S as compatible compared to HPG. On the other hand, THLE2 cells were received from ATCC at passage 38. As this is a high passage number to begin with, the cells may not be at the best performance and begin to lose function. Another point to consider is that THLE2 cells are immortalized primary cells by using viral vectors(72). Insertion of viral vectors may alter the expression of certain genes downstream. Both these factors are capable of influencing ASGPR expression in THLE2 cells and may contribute to the anomaly in the response curves.

Although, low K_m values of HPG+3S indicate receptor mediated internalization, uptake through ASGPR was confirmed through experiments performed with HEK293 cells ectopically expressing ASGPR1 and ASGPR2 genes. The results of this experiment indicate that internalization of HPG+3S can take place even if ASGPR1 gene is present and does not rely much on ASGPR2 gene. Competitive inhibition studies show that HPG+3S has a better affinity for the receptor as it takes a 1:4 ratio of HPG+3S to asialofetuin to show at least 50% inhibition.

The 85% inhibition seen with GalNAc is with a 10000-fold increase. The difference in competitive inhibition between asialofetuin and GalNAc is explained with their difference in the range of IC₅₀ values of the receptor (Asialofetuin: 45.6 μM; GalNAc: 4.55 mM)(54).

Initially efflux experiments were designed to be measured using a spectrofluorometer, but its sensitivity was not high enough to detect the expected nanomolar (or less than nano level) concentration of the polymer effluxed out hepatocytes. An alternate route was chosen where we could indirectly detect efflux of the polymer. We do not see a difference between HPG and blank since the cells were treated only for 2 hours. From the initial time response graphs (Figure16), we know that there is very little uptake of HPG compared to HPG+3S. There are a few drawbacks with this experiment, the first one being the cleavage of polymer can happen at any position or may not happen at all (hepatocytes are known for intact transport of cargo (77)). For example, the dye tagged region of polymer could still be within the cell, resulting in detection of positive cells, but there is a high possibility for the rest of the polymer to be effluxed out and vice versa. Secondly, after changing the cells to fresh media, the media was not changed. This means that whatever the polymer that was effluxed had a good chance of being available to the cells again for uptake. Even though the results of the efflux experiments could not be relied on, our animal studies data supports our hypothesis that the polymer not only can be internalized by the liver but can be excreted from the system as well. Approximately 17% of HPG+3S polymer (Figure 26B) that we found in feces in normal mice with functional kidneys supports that claim.

Monocytes were found to express both ASGPR1 and ASGPR2 genes (78). This naturally made us wonder if there will be an immune response against the polymer. Previous research on HPG suggested that HPG polymers of various size and shapes were biocompatible and found to have

no RBC aggregation or complement activation in mice after IV injections up to 28 days (40). Von Willebrand factor (VWF) is also considered to be a ligand for ASGPR (79) and its presence in monocytes could be involved in the clotting cascade mostly with clearance of VWF. Uptake by THP-1 (human monocyte line) of HPG+3S was significantly greater than HPG in our experiment, and this need not be seen only to illicit an immune response, but it might also aide in transporting of the polymer to the liver. It is also noteworthy that in vivo whole blood and spleen data show a significant difference between HPG+3S and HPG. It is difficult to draw any conclusions related to the physiological response to HPG+3S based on our data and hence further investigation is required. It is necessary to check long term hemocompatibility of HPG+3S if it is intended to replace glucose as an osmotic agent for peritoneal dialysis solutions and to begin with assays like PRT (plasma recalcification time) and APTT (Activated partial thromboplastin time) can be performed.

5.3 In vivo analysis: Biodistribution of HPG polymers in mice

Biodistribution results in mice were interesting and in congruence with our hypothesis. Uptake of HPG+3S by the liver served as a by-pass route of elimination of the polymer as seen in the feces and urine data. Liver uptake led to ~17% of HPG+3S excreted via feces even though the mice had normal functioning kidney. Elimination of the HPG+3S via feces led to drop in its content in urine within the first 8 hours, but more HPG+3S was eliminated between 8-24 hours than HPG. Hepatocytes have a robust rate of transcytosis from the sinusoidal surface to the canalicular surface and elucidates the rapid excretion of HPG+3S via the biliary route to feces (75,77). This indicates that the workload on the kidneys can be spread over a longer duration, which might be good news for patients with residual renal function. In the circulatory

system, the presence of HPG+3S in the whole blood was significantly more than HPG as per scintillation counts, but there was not a big difference in the percentage of polymer retained in both groups. By 48 hours, both the groups had less than 1% of polymer retained in the blood. This is a good sign that clearance of the polymer from the system will not be much of a problem. The concern here is that, the biodistribution results are based on a single intravenous injection to the mice, but in clinical scenario if HPG+3S were to replace glucose as the osmotic agent, then there would be constant absorption of HPG+3S in to the system and we need to study how polymer clearance would be under constant exposure to HPG+3S. Future experiments on rat models may help us understand the clearance of the polymer while administering HPG+3S daily via intra peritoneal injections. A few limitations of the animal study are that:

- 1) There were a few discrepancies in the collection of samples from mice. While collecting stomach and intestines, the contents of the gastrointestinal tract was excluded. Having that data would have provided more insights on where HPG+3S is present with respect to time and might have also helped explain the spike in gall bladder that we saw at 2 hours. Now, we have a gap in the passage since we see uptake by liver and elimination in feces.
- 2) Female C57BL/6 mice that were 7-8 weeks old were used in the study. The mice are still young and cannot be considered as fully matured adults. Young mice were preferred to avoid effects of hormonal changes on the metabolism of mice. However, metabolism in adult mice slows down when compared to younger mice and we know that end stage renal disease is more common in adults. The robust metabolism in the mice might not be what we would expect in older patients. Hence, these results cannot be extrapolated to clinical scenarios although they provide insights on HPG+3S metabolism.

- 3) The mice had normal functioning renal system. That would not be the case in clinical scenario. It is essential to see the biodistribution of both the control (HPG) and test (HPG+3s) polymer in mice with compromised renal function. Only then it would be able to understand the biological implications of HPG+3S.

Chapter 6: Summary and Future Studies

6.1 Summary

In this study, lower molecular weight HPG (3K) was successfully conjugated with GalNAc using sodium hydride and DMF. In vitro results show that there are two important factors that affect HPG polymer uptake by the hepatocytes:

1. The number of GalNAc sugars conjugated to HPG.
2. The number of receptors expressed on the cell surface.

The controllable factor would be the number of GalNAc sugars. Tagging too many GalNAc sugars would be ideal for HPG uptake by the liver, but caution must be taken to limit the size of the osmotic agent used for dialysis. Higher percentage solutions were needed for preparation of iso/hyper osmolar solution with increase in size. This can be expected to affect dwell times in the longer run.

Competitive inhibition studies show a decent affinity of HPG+3S to ASGPR when compared to asialofetuin. This solidified receptor mediated internalization of HPG+3S. The strengths of this study are that in vitro and in vivo results are in accordance and that HPG+3S shows good uptake in young mice with normal functioning urinary system. The fact that HPG+3S can target the liver with robust urinary clearance is a bonus to us and gives hope to expect a larger percentage of excretion via feces under diseased condition.

6.2 Recommended Future Studies

Here are a few directions to proceed from here:

- 1) Synthesizing HPG polymers with more GalNAc groups which could increase the efficiency of uptake. It would be best to optimize the synthesis of HPG-GalNAc polymers with the ability to regulate the number of GalNAc groups easily.
- 2) It was observed that the higher the molecular weight of HPG polymer, the greater the percentage of HPG solution. For this reason, it may be a better idea to see if 1K HPG can be used to conjugate 3 or more GalNAc sugars per molecule.
- 3) Under physiological conditions, other cell types in the liver will be involved and it will be a good idea to check the effect of HPG+3S on other liver cells such as Kupffer cells and stellate cells. Liver organoids containing stellate cells and hepatocytes (1:2 ratio) are available. Stellate cells when activated contribute to liver cirrhosis and it will be a good idea to check activation of stellate cells when exposed to HPG polymers(80–82).
- 4) Since HPG+3S shows quite a strong affinity to the receptor, it would be a good idea to check if injection of HPG+3S in mice will affect the clearance of other glycosylated proteins in the system (for example: VWF and other clotting factors).
- 5) Peritoneal membrane health is important for ultrafiltration. Human peritoneal membrane cells can be used to check toxicity of HPG-GalNAc polymers and animal studies can be done to check thickening of peritoneal membrane and apoptosis of peritoneal membrane cells.
- 6) Although hemocompatibility of HPG (higher molecular weight) has previously been performed, lower molecular weight HPG conjugated with GalNAc may behave completely differently. Since, we are considering HPG+3S as an osmotic agent to

replace glucose in future, long term hemocompatibility and bio compatibility tests should be performed.

- 7) Biodistribution study of HPG polymers in mice with compromised renal function.
- 8) Intra peritoneal injections for longer study durations in mice or rats with compromised renal function (such as 5/6 nephrectomy) should be done and ultrafiltration should be calculated.

Bibliography

1. Kidney Failure: Symptoms, Causes & Diagnosis - Urology Care Foundation [Internet]. [cited 2021 Feb 18]. Available from: [https://www.urologyhealth.org/urology-a-z/k/kidney-\(renal\)-failure](https://www.urologyhealth.org/urology-a-z/k/kidney-(renal)-failure)
2. Ronco C, Levin A, Warnock DG, Mehta RL, Kellum JA, Shah S, et al. Improving Outcomes from Acute Kidney Injury (AKI): Report on an Initiative. *Int J Artif Organs*. 2007 May 1;30(5):373–6.
3. Abbasi MA, Chertow GM, Hall YN. End-stage renal disease. *BMJ Clin Evid* [Internet]. 2010 Jul 19 [cited 2020 Sep 17];2010. Available from: <https://www.ncbi.nlm.nih.gov/pmc/articles/PMC3217820/>
4. Travers K, Martin A, Khankhel Z, Boye KS, Lee LJ. Burden and management of chronic kidney disease in Japan: systematic review of the literature. *Int J Nephrol Renov Dis*. 2013 Jan 3;6:1–13.
5. Introduction to Volume One: 2012 USRDS Annual Data Report Atlas of Chronic Kidney Disease in the United States- ClinicalKey [Internet]. [cited 2021 Mar 12]. Available from: <https://www-clinicalkey-com.ezproxy.library.ubc.ca/#!/content/playContent/1-s2.0-S0272638612013479?returnurl=null&referrer=null>
6. Arora P, Vasa P, Brenner D, Iglar K, McFarlane P, Morrison H, et al. Prevalence estimates of chronic kidney disease in Canada: results of a nationally representative survey. *CMAJ*. 2013 Jun 11;185(9):E417–23.
7. Zelman JL. The economic burden of end-stage renal disease in Canada. *Kidney Int*. 2007 Nov 1;72(9):1122–9.

8. Komenda P, Yu N, Leung S, Bernstein K, Blanchard J, Sood M, et al. Secular trends in end-stage renal disease requiring dialysis in Manitoba, Canada: a population-based study. *CMAJ Open*. 2015 Jan 13;3(1):E8–14.
9. Gao A, Osgood ND, Jiang Y, Dyck RF. Projecting prevalence, costs and evaluating simulated interventions for diabetic end stage renal disease in a Canadian population of aboriginal and non-aboriginal people: an agent based approach. *BMC Nephrol* [Internet]. 2017 Sep 4 [cited 2021 May 8];18. Available from: <https://www.ncbi.nlm.nih.gov/pmc/articles/PMC5584022/>
10. Annual Statistics on Organ Replacement in Canada: Dialysis, Transplantation and Donation, 2008 to 2017. 2008;9.
11. Agarwal R. Defining end-stage renal disease in clinical trials: a framework for adjudication. *Nephrol Dial Transplant*. 2016 Jun 1;31(6):864–7.
12. Peterson JC, Adler S, Burkart JM, Greene T, Hebert LA, Hunsicker LG, et al. Blood pressure control, proteinuria, and the progression of renal disease. The Modification of Diet in Renal Disease Study. *Ann Intern Med*. 1995 Nov 15;123(10):754–62.
13. Klag MJ, Whelton PK, Randall BL, Neaton JD, Brancati FL, Ford CE, et al. Blood pressure and end-stage renal disease in men. *N Engl J Med*. 1996 Jan 4;334(1):13–8.
14. Brancati FL, Whelton PK, Randall BL, Neaton JD, Stamler J, Klag MJ. Risk of end-stage renal disease in diabetes mellitus: a prospective cohort study of men screened for MRFIT. Multiple Risk Factor Intervention Trial. *JAMA*. 1997 Dec 17;278(23):2069–74.
15. Iseki K, Ikemiya Y, Iseki C, Takishita S. Proteinuria and the risk of developing end-stage renal disease. *Kidney Int*. 2003 Apr;63(4):1468–74.

16. Locatelli F, Pozzoni P, Vecchio LD. Renal Replacement Therapy in Patients with Diabetes and End-Stage Renal Disease. *J Am Soc Nephrol*. 2004 Jan 1;15(1 suppl):S25–9.
17. Hemodialysis | NEJM [Internet]. *New England Journal of Medicine*. [cited 2021 Mar 1]. Available from: <https://www-nejm-org.ezproxy.library.ubc.ca/doi/full/10.1056/NEJMra0902710>
18. Meyer TW, Hostetter TH. Uremia. *N Engl J Med*. 2007 Sep 27;357(13):1316–25.
19. Locatelli F, Manzoni C, Di Filippo S. The importance of convective transport. *Kidney Int*. 2002 May 1;61:S115–20.
20. Suri RS, Nesrallah GE, Mainra R, Garg AX, Lindsay RM, Greene T, et al. Daily Hemodialysis: A Systematic Review. *Clin J Am Soc Nephrol*. 2006 Jan 1;1(1):33–42.
21. Masterson R. The advantages and disadvantages of home hemodialysis. *Hemodial Int*. 2008;12(s1):S16–20.
22. Abou Dagher G, Harmouche E, Jabbour E, Bachir R, Zebian D, Bou Chebl R. Sepsis in hemodialysis patients. *BMC Emerg Med* [Internet]. 2015 Oct 14 [cited 2021 Mar 1];15. Available from: <https://www.ncbi.nlm.nih.gov/pmc/articles/PMC4606908/>
23. Collins AJ, Hao W, Xia H, Ebben JP, Everson SE, Constantini EG, et al. Mortality risks of peritoneal dialysis and hemodialysis. *Am J Kidney Dis*. 1999 Dec 1;34(6):1065–74.
24. Sarnak MJ, Jaber BL. Mortality caused by sepsis in patients with end-stage renal disease compared with the general population. *Kidney Int*. 2000 Oct;58(4):1758–64.
25. Hansson JH, Watnick S. Update on Peritoneal Dialysis: Core Curriculum 2016. *Am J Kidney Dis*. 2016 Jan 1;67(1):151–64.
26. Peritoneal Dialysis | NIDDK [Internet]. *National Institute of Diabetes and Digestive and Kidney Diseases*. [cited 2021 Mar 2]. Available from: <https://www.niddk.nih.gov/health-information/kidney-disease/kidney-failure/peritoneal-dialysis>

27. Beaudry A, Ferguson TW, Rigatto C, Tangri N, Dumanski S, Komenda P. Cost of Dialysis Therapy by Modality in Manitoba. *Clin J Am Soc Nephrol*. 2018 Aug 7;13(8):1197–203.
28. Karopadi AN, Mason G, Rettore E, Ronco C. Cost of peritoneal dialysis and haemodialysis across the world. *Nephrol Dial Transplant*. 2013 Oct 1;28(10):2553–69.
29. Cost Comparison of Peritoneal Dialysis Versus Hemodialysis in End-Stage Renal Disease [Internet]. *AJMC*. [cited 2020 May 22]. Available from: https://www.ajmc.com/journals/issue/2009/2009-08-vol15-n8/ajmc_09augberger_509to518
30. Klarenbach SW, Tonelli M, Chui B, Manns BJ. Economic evaluation of dialysis therapies. *Nat Rev Nephrol*. 2014 Nov;10(11):644–52.
31. Yung S, Chan TM. Pathophysiology of the Peritoneal Membrane during Peritoneal Dialysis: The Role of Hyaluronan. *J Biomed Biotechnol* [Internet]. 2011 [cited 2021 Mar 2];2011. Available from: <https://www.ncbi.nlm.nih.gov/pmc/articles/PMC3238805/>
32. Kawaguchi Y, Hasegawa T, Nakayama M, Kubo H. Issues affecting the longevity of the continuous peritoneal dialysis therapy. *Kidney Int Suppl*. 1997 Nov 1;62:S105.
33. Saxena R. Pathogenesis and treatment of peritoneal membrane failure. *Pediatr Nephrol*. 2008 May 1;23(5):695–703.
34. Mortier S, Faict D, Schalkwijk CG, Lameire NH, De Vriese ANS. Long-term exposure to new peritoneal dialysis solutions: Effects on the peritoneal membrane. *Kidney Int*. 2004 Sep 1;66(3):1257–65.
35. Kim Y-L, Cho J-H, Choi J-Y, Kim C-D, Park S-H. Systemic and local impact of glucose and glucose degradation products in peritoneal dialysis solution. *J Ren Nutr Off J Counc Ren Nutr Natl Kidney Found*. 2013 May;23(3):218–22.

36. García-López E, Lindholm B, Davies S. An update on peritoneal dialysis solutions. *Nat Rev Nephrol.* 2012 Feb 21;8:224–33.
37. Sunder A, Hanselmann R, Frey H, Mülhaupt R. Controlled Synthesis of Hyperbranched Polyglycerols by Ring-Opening Multibranching Polymerization. *Macromolecules.* 1999 Jun;32(13):4240–6.
38. Frey H, Haag R. Dendritic polyglycerol: a new versatile biocompatible material. *Rev Mol Biotechnol.* 2002 May 1;90(3):257–67.
39. Wilms D, Stiriba S-E, Frey H. Hyperbranched Polyglycerols: From the Controlled Synthesis of Biocompatible Polyether Polyols to Multipurpose Applications. *Acc Chem Res.* 2010 Jan 19;43(1):129–41.
40. Kainthan RK, Janzen J, Levin E, Devine DV, Brooks DE. Biocompatibility Testing of Branched and Linear Polyglycidol. *Biomacromolecules.* 2006 Mar 1;7(3):703–9.
41. Kainthan RK, Hester SR, Levin E, Devine DV, Brooks DE. In vitro biological evaluation of high molecular weight hyperbranched polyglycerols. *Biomaterials.* 2007 Nov 1;28(31):4581–90.
42. Kainthan RK, Brooks DE. In vivo biological evaluation of high molecular weight hyperbranched polyglycerols. *Biomaterials.* 2007 Nov;28(32):4779–87.
43. Abbina S, Vappala S, Kumar P, Siren EMJ, La CC, Abbasi U, et al. Hyperbranched polyglycerols: recent advances in synthesis, biocompatibility and biomedical applications. *J Mater Chem B.* 2017 Dec 6;5(47):9249–77.
44. Li S, Huang Z, Li X, Zhao Y, Jiang X, Wen Y, et al. Evaluation of hyperbranched polyglycerol for cold perfusion and storage of donor kidneys in a pig model of kidney autotransplantation. *J Biomed Mater Res B Appl Biomater.* 2020 Oct 24;e34750.

45. Kainthan RK, Janzen J, Kizhakkedathu JN, Devine DV, Brooks DE. Hydrophobically derivatized hyperbranched polyglycerol as a human serum albumin substitute. *Biomaterials*. 2008 Apr;29(11):1693–704.
46. Du C, Mendelson AA, Guan Q, Chapanian R, Chafeeva I, da Roza G, et al. The size-dependent efficacy and biocompatibility of hyperbranched polyglycerol in peritoneal dialysis. *Biomaterials*. 2014 Feb;35(5):1378–89.
47. Du C, Mendelson AA, Guan Q, Dairi G, Chafeeva I, da Roza G, et al. Hyperbranched polyglycerol is superior to glucose for long-term preservation of peritoneal membrane in a rat model of chronic peritoneal dialysis. *J Transl Med*. 2016 Dec;14(1):338.
48. Han BL, Guan Q, Chafeeva I, Mendelson AA, Roza G da, Liggins R, et al. Peritoneal and Systemic Responses of Obese Type II Diabetic Rats to Chronic Exposure to a Hyperbranched Polyglycerol-Based Dialysis Solution. *Basic Clin Pharmacol Toxicol*. 2018;123(4):494–503.
49. D'Souza AA, Devarajan PV. Asialoglycoprotein receptor mediated hepatocyte targeting - strategies and applications. *J Control Release Off J Control Release Soc*. 2015 Apr 10;203:126–39.
50. Li Y, Huang G, Diakur J, Wiebe LI. Targeted delivery of macromolecular drugs: asialoglycoprotein receptor (ASGPR) expression by selected hepatoma cell lines used in antiviral drug development. *Curr Drug Deliv*. 2008 Oct 1;5(4):299.
51. Bischoff J, Libresco S, Shia MA, Lodish HF. The H1 and H2 polypeptides associate to form the asialoglycoprotein receptor in human hepatoma cells. *J Cell Biol*. 1988 Apr 1;106(4):1067–74.

52. Meier M, Bider MD, Malashkevich VN, Spiess M, Burkhard P. Crystal Structure of the Carbohydrate Recognition Domain of the H1 Subunit of the Asialoglycoprotein Receptor. *J Mol Biol.* 2000 Jul;300(4):857–65.
53. Quintero-Martinez A. Assembly and selectivity of asialoglycoprotein receptors [Internet] [Ph.D.]. [England]: Imperial College London (United Kingdom); 2012 [cited 2021 Mar 7]. Available from: <http://search.proquest.com/docview/1557581996?pq-origsite=summon>
54. O K, D S, O S, B C, B E. Trivalent, Gal/GalNAc-containing ligands designed for the asialoglycoprotein receptor. *Bioorg Med Chem.* 2008 Mar 7;16(9):5216–31.
55. Li M, Zhang W, Wang B, Gao Y, Song Z, Zheng QC. Ligand-based targeted therapy: a novel strategy for hepatocellular carcinoma. *Int J Nanomedicine.* 2016;11:5645–69.
56. Cho CS, GOTO M, Kobayashi A, Kobayashi K, Akaike T. Effect of ligand orientation on hepatocyte attachment onto the poly(N p-vinylbenzyl-o-β-D-galactopyranosyl-D-gluconamide) as a model ligand of asialoglycoprotein. *J Biomater Sci Polym Ed.* 1996 Jan 1;7(12):1097–104.
57. Tanowitz M, Hettrick L, Revenko A, Kinberger GA, Prakash TP, Seth PP. Asialoglycoprotein receptor 1 mediates productive uptake of N-acetylgalactosamine-conjugated and unconjugated phosphorothioate antisense oligonucleotides into liver hepatocytes. *Nucleic Acids Res.* 2017 Dec 1;45(21):12388–400.
58. Nair JK, Willoughby JLS, Chan A, Charisse K, Alam MdR, Wang Q, et al. Multivalent N-Acetylgalactosamine-Conjugated siRNA Localizes in Hepatocytes and Elicits Robust RNAi-Mediated Gene Silencing. *J Am Chem Soc.* 2014 Dec 10;136(49):16958–61.
59. Chan A, Liebow A, Yasuda M, Gan L, Racie T, Maier M, et al. Preclinical Development of a Subcutaneous ALAS1 RNAi Therapeutic for Treatment of Hepatic Porphyrrias Using Circulating RNA Quantification. *Mol Ther - Nucleic Acids.* 2015 Jan 1;4:e263.

60. Willoughby JLS, Chan A, Sehgal A, Butler JS, Nair JK, Racie T, et al. Evaluation of GalNAc-siRNA Conjugate Activity in Pre-clinical Animal Models with Reduced Asialoglycoprotein Receptor Expression. *Mol Ther*. 2018 Jan;26(1):105–14.
61. Zimmermann TS, Karsten V, Chan A, Chiesa J, Boyce M, Bettencourt BR, et al. Clinical Proof of Concept for a Novel Hepatocyte-Targeting GalNAc-siRNA Conjugate. *Mol Ther*. 2017 Jan 4;25(1):71–8.
62. Reina J, Rioboo A, Montenegro J. Glycosyl Aldehydes: New Scaffolds for the Synthesis of Neoglycoconjugates via Bioorthogonal Oxime Bond Formation. *Synthesis*. 2018 Feb;50(04):831–45.
63. Staedtler AM, Hellmund M, Mehrabadi FS, Thota BNS, Zollner TM, Koch M, et al. Optimized effective charge density and size of polyglycerol amines leads to strong knockdown efficacy in vivo. *J Mater Chem B*. 2015 Nov 18;3(46):8993–9000.
64. User Guide: Protein Labeling Kits (For Alexa Fluor, Pacific Blue, Fluorescein-EX, and Oregon Green 488) [Internet]. [cited 2021 May 11]. Available from: https://www.thermofisher.com/document-connect/document-connect.html?url=https%3A%2F%2Fassets.thermofisher.com%2FTFS-Assets%2FSLSG%2Fmanuals%2FMAN0019835_AlexaFluor_ProteinLabelingKits_UG.pdf&title=VXNlciBHdWlkZTogUHJvdGVpbjBMYWJlbGluZyBLaXRzIChGb3IgQWxleGEgRmx1b3IsIFBhY2lmaWMgQmx1ZSwgRmx1b3Jlc2NlaW4tRVgsIGFuZCBPcmVnb24gR3JIZW4gNDg4KQ==
65. Chapanian R, Constantinescu I, Brooks DE, Scott MD, Kizhakkedathu JN. In vivo circulation, clearance, and biodistribution of polyglycerol grafted functional red blood cells. *Biomaterials*. 2012 Apr;33(10):3047–57.

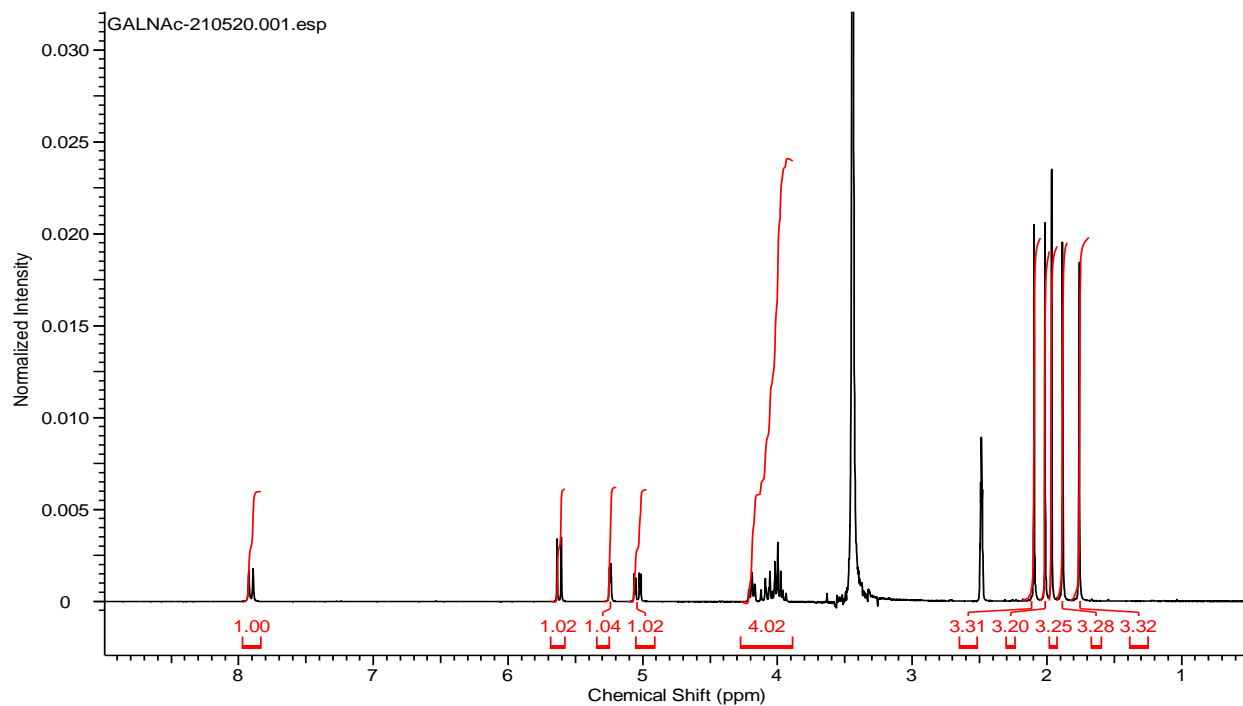
66. Hep G2 [HEPG2] ATCC® HB-8065™ [Internet]. [cited 2021 May 11]. Available from: <https://www.atcc.org/products/all/HB-8065.aspx#generalinformation>
67. Shirasago Y, Sekizuka T, Saito K, Suzuki T, Wakita T, Hanada K, et al. Isolation and Characterization of an Huh.7.5.1-Derived Cell Clone Highly Permissive to Hepatitis C Virus. *Jpn J Infect Dis.* 2015;68(2):81–8.
68. THLE-2 ATCC ® CRL-2706™ Homo sapiens liver/left lobe [Internet]. [cited 2021 May 11]. Available from: <https://www.atcc.org/products/all/CRL-2706.aspx>
69. Monestier M, Charbonnier P, Gateau C, Cuillel M, Robert F, Lebrun C, et al. ASGPR-Mediated Uptake of Multivalent Glycoconjugates for Drug Delivery in Hepatocytes. *Chembiochem Eur J Chem Biol.* 2016 Apr 1;17(7):590–4.
70. Dam TK, Gabius H-J, André S, Kaltner H, Lensch M, Brewer CF. Galectins Bind to the Multivalent Glycoprotein Asialofetuin with Enhanced Affinities and a Gradient of Decreasing Binding Constants †. *Biochemistry.* 2005 Sep;44(37):12564–71.
71. Farzan VM, Ulashchik EA, Martynenko-Makaev YV, Kvach MV, Aparin IO, Brylev VA, et al. Automated Solid-Phase Click Synthesis of Oligonucleotide Conjugates: From Small Molecules to Diverse *N*-Acetylgalactosamine Clusters. *Bioconjug Chem.* 2017 Oct 18;28(10):2599–607.
72. Pfeifer AM, Cole KE, Smoot DT, Weston A, Groopman JD, Shields PG, et al. Simian virus 40 large tumor antigen-immortalized normal human liver epithelial cells express hepatocyte characteristics and metabolize chemical carcinogens. *Proc Natl Acad Sci U S A.* 1993 Jun 1;90(11):5123–7.

73. Zhou Y, Teng P, Montgomery NT, Li X, Tang W. Development of Triantennary N-Acetylgalactosamine Conjugates as Degradable for Extracellular Proteins. *ACS Cent Sci*. 2021 Mar 24;7(3):499–506.
74. An Introduction to Biological Membranes | ScienceDirect [Internet]. [cited 2021 Apr 2]. Available from: <https://www.sciencedirect.com/book/9780444637727/an-introduction-to-biological-membranes>
75. Crawford JM. Role of Vesicle-Mediated Transport Pathways in Hepatocellular Bile Secretion. :21.
76. Schroeder B, McNiven MA. Importance of Endocytic Pathways in Liver Function and Disease. *Compr Physiol*. 2014 Oct;4(4):1403–17.
77. Schulze RJ, Schott MB, Casey CA, Tuma PL, McNiven MA. The cell biology of the hepatocyte: A membrane trafficking machine. *J Cell Biol*. :17.
78. Harris RL, van den Berg CW, Bowen DJ. ASGR1 and ASGR2, the Genes that Encode the Asialoglycoprotein Receptor (Ashwell Receptor), Are Expressed in Peripheral Blood Monocytes and Show Interindividual Differences in Transcript Profile. *Mol Biol Int* [Internet]. 2012 [cited 2020 Nov 16];2012. Available from: <https://www.ncbi.nlm.nih.gov/pmc/articles/PMC3419429/>
79. Grewal PK, Uchiyama S, Ditto D, Varki N, Le DT, Nizet V, et al. The Ashwell receptor mitigates the lethal coagulopathy of sepsis. *Nat Med*. 2008 Jun;14(6):648–55.
80. Schirmacher P, Geerts A, Pietrangelo A, Dienes HP, Rogler CE. Hepatocyte growth factor/hepatopoietin A is expressed in fat-storing cells from rat liver but not myofibroblast-like cells derived from fat-storing cells. *Hepatology*. 1992 Jan;15(1):5–11.

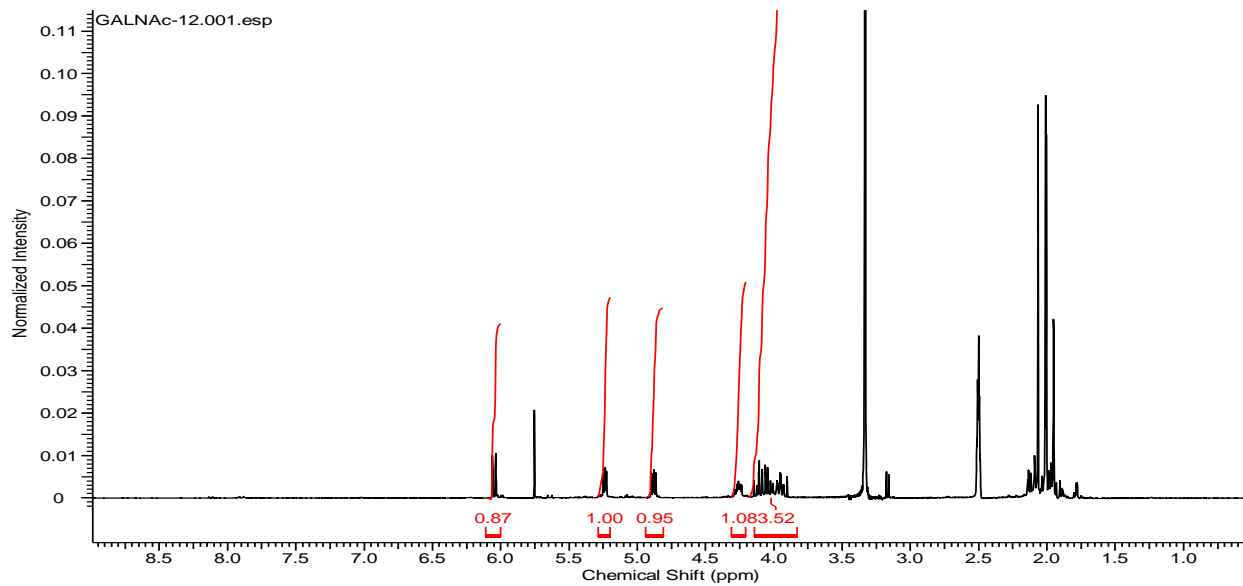
81. Abu-Absi SF, Hansen LK, Hu W-S. Three-dimensional co-culture of hepatocytes and stellate cells. *Cytotechnology*. 2004 Jul;45(3):125–40.
82. Kyffin JA, Sharma P, Leedale J, Colley HE, Murdoch C, Harding AL, et al. Characterisation of a functional rat hepatocyte spheroid model. *Toxicol In Vitro*. 2019 Mar;55:160–72.
83. Singh AP, Junemann A, Muthuraman A, Jaggi AS, Singh N, Grover K, et al. Animal models of acute renal failure. *Pharmacol Rep PR*. 2012;64(1):31–44.
84. Extraneal_EN.pdf [Internet]. [cited 2021 Apr 9]. Available from: https://www.baxter.ca/sites/g/files/ebysai1431/files/2018-11/Extraneal_EN.pdf
85. NUTRINEAL_EN.pdf [Internet]. [cited 2021 Apr 9]. Available from: https://www.baxter.ca/sites/g/files/ebysai1431/files/2018-11/NUTRINEAL_EN.pdf
86. Dianeal_EN.pdf [Internet]. [cited 2021 Apr 9]. Available from: https://www.baxter.ca/sites/g/files/ebysai1431/files/2018-11/Dianeal_EN.pdf
87. Physioneal_Viaflex_EN.pdf [Internet]. [cited 2021 Apr 9]. Available from: https://www.baxter.ca/sites/g/files/ebysai1431/files/2018-11/Physioneal_Viaflex_EN.pdf

Appendix

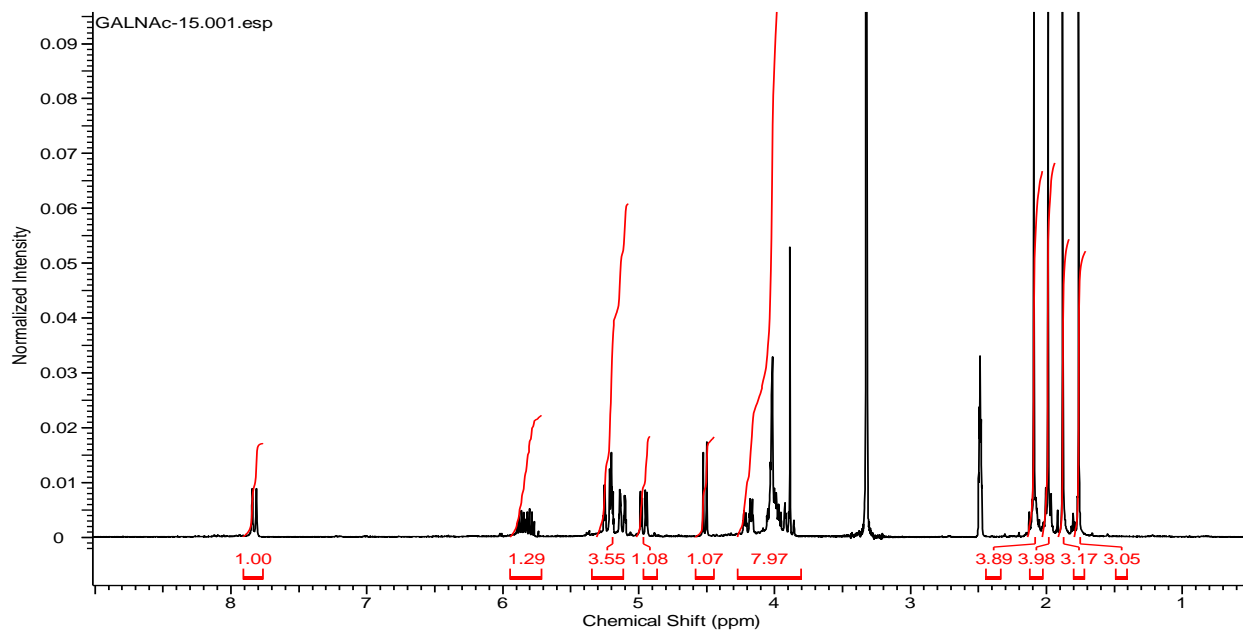
H NMR of intermediary products during sugar modification of GalNAc:



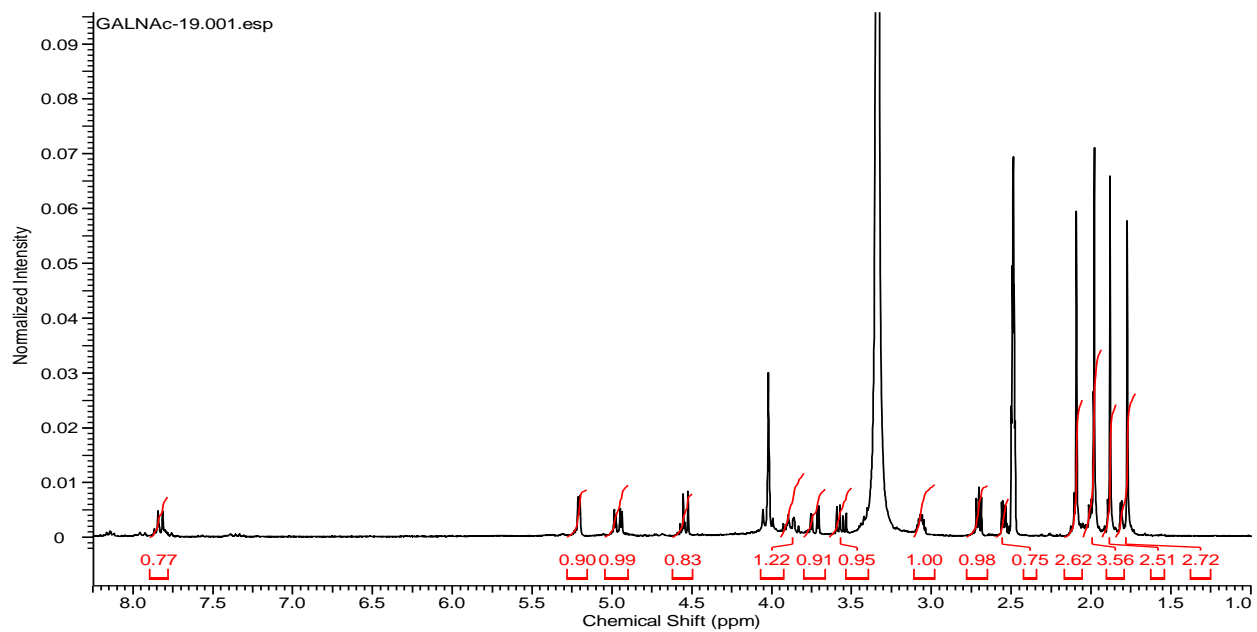
A) ¹H NMR spectrum of N-acetyl galactoseamine



B) ¹H NMR spectrum of D-galactopyrano-2-oxazoline



C) ¹H NMR spectrum of allyl GalNAc



D) ¹H NMR spectrum of GalNAc-epoxide